

Thesis

Submission date: 29-Jun-2021 03:25AM (UTC+0530)

Submission ID: 1613481744

File name: Thesis_3.pdf (7.68M)

Word count: 10923

Character count: 68036

**OPTIMIZATION OF PROCESS VARIABLE FOR ADDITIVE
MANUFACTURED PLA BASED TENSILE SPECIMEN USING
TAGUCHI DESIGN OF EXPERIMENT AND ARTIFICIAL NEURAL
NETWORK (ANN) TECHNIQUE**

A DISSERTATION

**SUBMITTED IN PARTIAL FULFILLMENT OF REQUIREMENTS
FOR THE AWARD OF THE DEGREE
OF**

**MASTER OF TECHNOLOGY
IN
PRODUCTION ENGINEERING**

Submitted by

RISHABH TEHARIA

2K19/PIE/10

Under the supervision of

PROF. RANGANATH M SINGARI

DR. HARISH KUMAR



DEPARTMENT OF MECHANICAL ENGINEERING

DELHI TECHNOLOGICAL UNIVERSITY

(Formerly Delhi College of Engineering)

Bawana Road, Delhi-110042

June 2021

DELHI TECHNOLOGICAL UNIVERSITY

(Formerly Delhi College of Engineering)

Bawana road, Delhi-11042

CANDIDATE'S DECLARATION

I RISHABH TEHARIA, Roll no-2k19/PIE/10 student of MTech (Production Engineering), hereby declare that the project dissertation titled “ Optimization of process variable for additive manufactured PLA based tensile specimen using Taguchi design of Experiment and Artificial Neural Network (ANN) technique” which is submitted by me to the Department of Mechanical Engineering, Delhi Technological University, Delhi in partial fulfilment of the requirement for the award of the degree of the Master of technology, is original and not copied from any source without proper citation. This work has not previously formed the basis for the award of any Degree, Diploma Associateship, Fellowship or other similar title or recognition

Place: Delhi

(RISHABH TEHARIA)

Date:

DELHI TECHNOLOGICAL UNIVERSITY

(Formerly Delhi College of Engineering)

Bawana Road, Delhi-110042

CERTIFICATE

I hereby certify that the project Dissertation titled “OPTIMIZATION OF PROCESS VARIABLE FOR ADDITIVE MANUFACTURED PLA BASED TENSILE SPECIMEN USING TAGUCHI DESIGN OF EXPERIMENT AND ARTIFICIAL NEURAL NETWORK (ANN) TECHNIQUE” which is submitted by, roll no 2k19/PIE/10, Delhi Technological University, Delhi in partial fulfilment of the requirement for the award of degree of Master of Technology, is a record of the project work carried out by the student under my supervision. To the best of my knowledge this work has not been submitted in part or full for any Degree or Diploma to this university or elsewhere.

Place: Delhi

Date:

Prof. RANGANATH M. SINGARI
Head, Department of Design
Delhi Technological University
DELHI-110042

Place: Delhi

Date:

Prof. Harish Kumar
Department of Mechanical Engineering
National Institute of Technology, Delhi
DELHI-110040

ABSTRACT

Additive Manufacturing or 3-D printing is a fabrication process by which a 3-dimensional solid object is manufactured by depositing layers by layers on the object. It is emerging as one of the innovative technologies and highly affect the manufacturing system. Today, additive manufacturing (AM) reveals changes in complete value creation, strategic system, and processes. Mass customization with minimization of waste and ability to manufacture complex structure make this process superior over other. Freedoms of design, rapid prototyping are some other benefits.

The aim of this study is to optimize the process parameters of fused deposition modeling (FDM) by exploring the tensile testing of Polylactic acid (PLA). In this work, we varied process parameters like layer thickness, raster orientation, structure, speed, and nozzle temperature are investigated. Based on these parameters Tensile specimen are printed by using Fusebot 250+ FDM. The Tensile behavior was investigated under different condition. Using Artificial Neural Network, the obtained experimental results are validated and checked for optimum value of tensile strength under defined conditions.

ACKNOWLEDGEMENT

It is a matter of great pleasure for me to present my dissertation report on “Optimization of process variable for additive manufactured PLA based tensile specimen using Taguchi design of Experiment and Artificial Neural Network (ANN) technique”. First and foremost, I am profoundly grateful to my guides Prof. Ranganath M. Singari, Department of mechanical, Production and Industrial Engineering, Delhi technological University, Delhi and Dr. Harish Kumar, Head of Department of mechanical engineering, National Institute of Technology, Delhi for their expert guidance and continuous encouragement during all states of thesis. I feel lucky to get an opportunity to work with them, I am thankful to the kindness and generosity shown by them towards me, as it helped me morally complete the project before starting it. Last, but not the least, I would like to thank my family members for their help, encouragement, and prayers through all these months. I dedicate my work to them.

Place: Delhi

RISHABH TEHARIA

Date:

13
Table of Contents

| | |
|---|-----------|
| CANDIDATE'S DECLARATION | 2 |
| CERTIFICATE | 3 |
| ABSTRACT | 4 |
| ACKNOWLEDGEMENT | 5 |
| LIST OF FIGURES | 8 |
| LIST OF TABLES | 9 |
| LIST OF GRAPHS..... | 10 |
| LIST OF ABBREVIATIONS | 12 |
| 19 CHAPTER 1 | 13 |
| INTRODUCTION..... | 13 |
| 1.1. Overview..... | 13 |
| 1.2. History..... | 14 |
| 1.3. Process of 3-d printing..... | 15 |
| 1.4. Methods of additive manufacturing..... | 17 |
| 1.5. Materials | 18 |
| 1.6. Application and challenges | 20 |
| 1.7. Fused Deposition Modelling..... | 23 |
| 1.8. Process Parameters | 24 |
| CHAPTER 2 | 27 |
| LITERATURE REVIEW..... | 27 |
| CHAPTER 3 | 32 |
| MODELLING AND FABRICATION OF TEST SPECIMENS..... | 32 |
| 3.1. Modeling..... | 32 |

| | |
|---|-----------|
| 3.2. Selection of Process Parameters | 33 |
| 3.3. Orthogonal array | 34 |
| 3.4. Fabrication and Experimental Setup..... | 35 |
| 3.5. Artificial Neural Network | 37 |
| CHAPTER 4 | 39 |
| TESTING AND EXPERIMENTAL SETUP..... | 39 |
| CHAPTER 5 | 68 |
| ANALYSIS AND CALCULATIONS OF OPTIMUM VALUE | 68 |
| 5.1 Taguchi Analysis | 68 |
| 5.2 Artificial Neural Network (ANN) | 71 |
| CHAPTER 6 | 76 |
| CONCLUSION..... | 76 |
| REFERENCES | 77 |

LIST OF FIGURES

| | | |
|-----------|---|----|
| Figure 1 | A geometry-material-machine-process roadmap for AM and Maker Movement | 14 |
| Figure 2 | Printing procedure | 16 |
| Figure 3 | Process of 3-D printing | 17 |
| Figure 4 | Dimensions of Tensile Test Specimen | 32 |
| Figure 5 | STL and CAD model of Tensile Test Specimen | 33 |
| Figure 6 | Fusebot 250+ | 36 |
| Figure 7 | TKG EC 50 | 36 |
| Figure 8 | Fabricated Samples | 37 |
| Figure 9 | Experimental setup during and after test | 39 |
| Figure 10 | Sample after testing | 40 |
| Figure 11 | Main effects plot for S/N Ratios | 70 |
| Figure 12 | Main effect for Means Plot using MINITAB | 71 |
| Figure 13 | Structure of ANN developed using MATLAB | 71 |
| Figure 14 | Regression plot of Artificial Neural Network | 73 |
| Figure 15 | Error histogram | 73 |
| Figure 16 | Training plot | 74 |
| Figure 17 | Performance plot | 74 |

LIST OF TABLES

| | |
|--|----|
| Table 1: History of 3-D printing | 15 |
| Table 2 Different processes of additive manufacturing | 17 |
| 12 Table 3 A summary of main applications, benefits, and challenges of the main materials for additive manufacturing | 18 |
| Table 4 Additive manufacturing process types with applications | 20 |
| Table 5 Application of 3-D printing | 22 |
| Table 6 Taguchi L27 Orthogonal Array | 34 |
| Table 7 Experimental Results | 68 |
| 11 Table 8 Response Table for Signal to Noise Ratios | 69 |
| Table 9 Response Table for Means | 70 |
| Table 10 Comparison of Experimental and ANN Predicted UTS Strength | 71 |

LIST OF GRAPHS

| | |
|---|----|
| Graph 1 Experimental load- displacement graph of sample 1 | 41 |
| Graph 2 Experimental Stress- Strain graph of sample 1 | 41 |
| Graph 3 Experimental load- displacement graph of sample 2 | 42 |
| Graph 4 Experimental Stress- Strain graph of sample 2 | 42 |
| Graph 5 Experimental load- displacement graph of sample 3 | 43 |
| Graph 6 Experimental Stress- Strain graph of sample 3 | 43 |
| Graph 7 Experimental load- displacement graph of sample 4 | 44 |
| Graph 8 Experimental Stress- Strain graph of sample 4 | 44 |
| Graph 9 Experimental load- displacement graph of sample 5 | 45 |
| Graph 10 Experimental Stress- Strain graph of sample 5 | 45 |
| Graph 11 Experimental load- displacement graph of sample 6 | 46 |
| Graph 12 Experimental Stress- Strain graph of sample 6 | 46 |
| Graph 13 Experimental load- displacement graph of sample 7 | 47 |
| Graph 14 Experimental Stress- Strain graph of sample 7 | 47 |
| Graph 15 Experimental load- displacement graph of sample 8 | 48 |
| Graph 16 Experimental Stress- Strain graph of sample 8 | 48 |
| Graph 17 Experimental load- displacement graph of sample 9 | 49 |
| Graph 18 Experimental Stress- Strain graph of sample 9 | 49 |
| Graph 19 Experimental load- displacement graph of sample 10 | 50 |
| Graph 20 Experimental Stress- Strain graph of sample 10 | 50 |
| Graph 21 Experimental load- displacement graph of sample 11 | 51 |
| Graph 22 Experimental Stress- Strain graph of sample 11 | 51 |
| Graph 23 Experimental load- displacement graph of sample 12 | 52 |
| Graph 24 Experimental Stress- Strain graph of sample 12 | 52 |
| Graph 25 Experimental load- displacement graph of sample 13 | 53 |
| Graph 26 Experimental Stress- Strain graph of sample 13 | 53 |
| Graph 27 Experimental load- displacement graph of sample 14 | 54 |
| Graph 28 Experimental Stress- Strain graph of sample 14 | 54 |
| Graph 29 Experimental load- displacement graph of sample 15 | 55 |
| Graph 30 Experimental Stress- Strain graph of sample 15 | 55 |
| Graph 31 Experimental load- displacement graph of sample 16 | 56 |
| Graph 32 Experimental Stress- Strain graph of sample 16 | 56 |
| Graph 33 Experimental load- displacement graph of sample 17 | 57 |
| Graph 34 Experimental Stress- Strain graph of sample 17 | 57 |
| Graph 35 Experimental load- displacement graph of sample 18 | 58 |

| | |
|---|----|
| Graph 36 Experimental Stress- Strain graph of sample 18 | 58 |
| Graph 37 Experimental load- displacement graph of sample 19 | 59 |
| Graph 38 Experimental Stress- Strain graph of sample 19 | 59 |
| Graph 39 Experimental load- displacement graph of sample 20 | 60 |
| Graph 40 Experimental Stress- Strain graph of sample 20 | 60 |
| Graph 41 Experimental load- displacement graph of sample 21 | 61 |
| Graph 42 Experimental Stress- Strain graph of sample 21 | 61 |
| Graph 43 Experimental load- displacement graph of sample 22 | 62 |
| Graph 44 Experimental Stress- Strain graph of sample 22 | 62 |
| Graph 45 Experimental load- displacement graph of sample 23 | 63 |
| Graph 46 Experimental Stress- Strain graph of sample 23 | 63 |
| Graph 47 Experimental load- displacement graph of sample 24 | 64 |
| Graph 48 Experimental Stress- Strain graph of sample 24 | 64 |
| Graph 49 Experimental load- displacement graph of sample 25 | 65 |
| Graph 50 Experimental Stress- Strain graph of sample 25 | 65 |
| Graph 51 Experimental load- displacement graph of sample 26 | 66 |
| Graph 52 Experimental Stress- Strain graph of sample 26 | 66 |
| Graph 53 Experimental load- displacement graph of sample 27 | 67 |
| Graph 54 Experimental Stress- Strain graph of sample 27 | 67 |

LIST OF ABBREVIATIONS

| | |
|-------------|---|
| 3D | Three Dimensional |
| PLA | Poly lactic Aid |
| ABS | ¹⁴ Acrylonitrile Butadiene Styrene |
| AM | Additive Manufacturing |
| ANN | Artificial Neural Network |
| ASTM | American Society for Testing and Materials |
| CAD | Computer Aided Design |
| DoF | Degree of Freedom |
| FDM | Fused Deposition Modelling |
| S/N | Signal to Noise |
| STL | Standard Tessellation Language |
| UTM | Universal Testing Machine |
| UTS | Ultimate Tensile Strength |

CHAPTER 1

INTRODUCTION

1.1. Overview

Advancements in computational capabilities have paved new roads for development in the field of manufacturing industries. The manufacturing industries all around the globe are observing a gradual shift or transformation in the philosophy, which is used to manufacture a product. With the implementations of manufacturing systems such as Agile Manufacturing System which targets specifically dynamic and volatile markets, a need to bring products to market as quickly as possible was a key challenge, to stay unbeaten in the competitive market. Additive Manufacturing was introduced to cut down the time required to bring any product to market as quickly as possible by finalizing designs for manufacturing.

Conventional manufacturing methodologies are enveloped in idea of removing material from a preformed raw shape or raw material and generate a desired shape. Though, it is widely accepted and used idea to manufacture any product, it has some serious challenges when it comes to manufacturing complex geometric shapes. Additive Manufacturing, on the other hand works on the opposite idea i.e. adding material in a predefined manner to generate a final shape. Additive Manufacturing is a rapidly emerging manufacturing ideology which is being adopted widely in aviation and medical.

Additive manufacturing (AM) is a technique used for fabricating a wide range of structures and complex geometries from three-dimensional (3D) model data. AM is a process for making a 3D object of desired shape from a 3D model or other electronic data sources

through additive processes in which successive layers of material are laid down under computer controls.

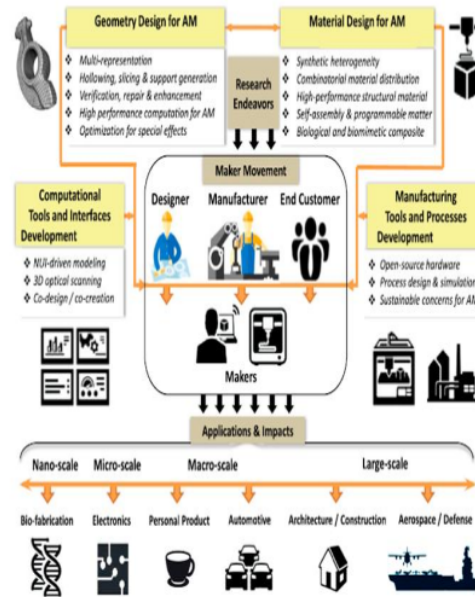


Figure 1 A geometry-material-machine-process roadmap for AM and Maker Movement

1.2. History

The history of 3-D printing is a science which is just 4 decades old. The radical growth of scientific, engineering, and technological research has brought to its mature level. 3-D printing technology's historical advances may be represented by various perspectives such as period, specific features, and application. Several historians divided various periods of history into

- ❖ Infancy Period: 1981 to 1999
- ❖ Spring Period: 1999 to 2010
- ❖ Mature Period: 2011 to present

From starting till consideration duration of its existence, 3-D printers were too expensive, but now the cost has dropped to \$500-\$1000 which make it affordance product.

Table 1: History of 3-D printing

| YEAR | DESCRIPTION OF EVENT |
|------------|---|
| 1984 | Stereolithography invented by Chuck Hull |
| 1990 | 3-D printing is commercialized by Stratasys and called it as fused deposition modelling (FSM) |
| 1999 | Researcher 3-D print the scaffolding for a new bladder then grow cells on it. |
| 2002 | First kidney of animal was printed |
| 2005 | RepRap founded with the goal to creating a free/open source printer that can replicate itself |
| 2010 | First time human blood vessel is printed by Organovo |
| March 2014 | First 3-D printed skull transplant was done in Norway |
| April 2014 | 2000 sq. ft. houses are printed by Chinese company using 3-D printer |

1.3. Process of 3-d printing

❖ Creation of virtual model

Modelling software's such as AutoCAD, solid work's, Catia etc. are used to make virtual models of component. Design engineers provides the data to create the designs or may obtain designs from existing designs. ANSYS, COMSOL, ABAQUS are some analyzing software's that are used for virtual analysis of the object before production. Reverse engineering is also used for creation of models. With the help of UV light scanning of the objects are done i.e., UV light form source hit the target and received back to get scanned.

❖ Understanding the functional part

Designers create the functional parts which are unique structures. The spacing between the parts should be done precision by the designers. Single parts are created by AM process which are further combined to get whole assembly.

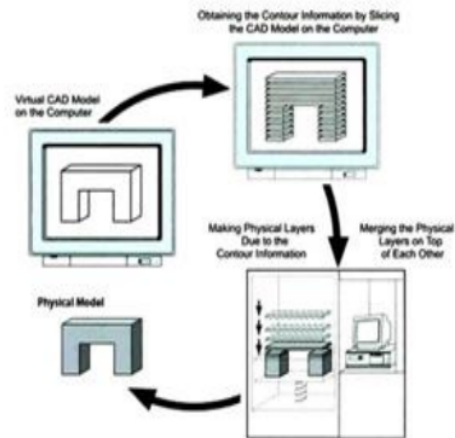


Figure 2 Printing procedure

❖ Convert into STL

Standard triangle language (STL) is used for the sliding process. So, for this reason models are converted into STL. STL file mainly describe the main attributes i.e. surface geometry of design file. Design file is transformed into **triangulated surface** using three dimensional Cartesian co-ordinates.

❖ Slicing and creating support

From STL file, contour data is created. As per layer thickness, slicing process is set horizontally. Uniformity is maintained while slicing the materials. Geometry and capability of machine are important factor that determines the thickness of slicing process.

❖ Export to G-code file

G-CODE is created by slicing software for the 3-D printing process. The G-CODE is symmetrical of the CNC machine coding process. The movement of extruder head and platform direction is provided by the coding. In some machine platform is fixed and the extruder moves in all 3 dimensions but in some machines only platforms moves in z direction. All these movements are control by the g-code.

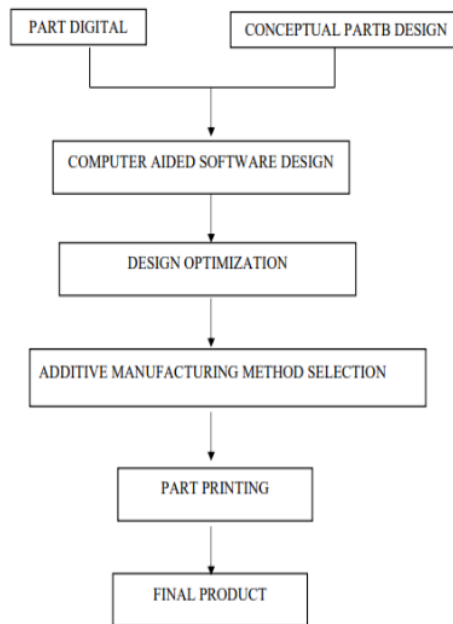


Figure 3 Process of 3-D printing

1.4. Methods of additive manufacturing

Additive manufacturing techniques have been developed to satisfy the need for the fine-resolution printing of complex structures. Rapid prototyping, the potential to print massive objects, reduce printing faults, and improve mechanical properties are some of the main factors driving AM technology growth.

Table 2 Different processes of additive manufacturing

| METHODS | MATERIAL | BENEFITS | APPLICATION |
|-------------------|------------------------------------|--|---|
| Stereolithography | A resin with photo active monomers | <ul style="list-style-type: none"> • High Resolution • Excellent Quality | <ul style="list-style-type: none"> • Used in prototyping • Biomedical |

| | | | |
|--------------------------------------|--|---|--|
| Powder bed fusion | Compacted fine powder metal, Limited polymers Alloys | <ul style="list-style-type: none"> • Aerospace • Biomedical • Light weight-structure • Biomedical | <ul style="list-style-type: none"> • High resolution • Excellent quality |
| Inkjet printing and contour crafting | In a liquid ceramic, a concentrated dispersion of particles | <ul style="list-style-type: none"> • Building • Biomedical • Large structure | <ul style="list-style-type: none"> • Reduce cost • Reduce time • Excellent mechanical properties |
| Fused deposition modelling | Continuous strand of thermoplastic polymers | <ul style="list-style-type: none"> • Advanced composition parts • Rapid prototyping | <ul style="list-style-type: none"> • Less expensive • Uniformity • Speedy |
| Direct energy deposition | Metal and alloys in the form of powder or wire ceramics and polymers | <ul style="list-style-type: none"> • Cladding • Biomedical • Retrofitting • Aerospace | <ul style="list-style-type: none"> • Less expensive • Limited time • Accurate composition control |

The table above describe the different methods that are used in 3-D printing technology. The main methods used in additive manufacturing technology are stereolithography, powder bed fusion, direct energy deposition, fused deposition modelling and inkjet printing. The limitations, materials, and benefits of all these processes have been discussed in table 3.

1.5. Materials

The list of materials used in additive manufacturing are:

Table 3 A summary of main applications, benefits, and challenges of the main materials for additive manufacturing

| MATERIAL | APPLICATIONS | BENEFITS | CHALLENGES |
|-----------------------|--|--|---|
| Metals and Alloys | <ul style="list-style-type: none"> • Military • Biomedical • Automotive • Aerospace | <ul style="list-style-type: none"> • Multifunctional optimization • Mass customization • Reduce wastage of material • Fewer assembly Components • Possibility to repair parts | <ul style="list-style-type: none"> • Limited selection of alloys • Dimensional inaccuracy • Surface finish is poor • Required post processing |
| Polymers & Composites | <ul style="list-style-type: none"> • Aerospace • Automotive • Sports • Medical • Architecture • Toys • Biomedical | <ul style="list-style-type: none"> • Fast prototyping • Cost effective • Complex structure • Mass-customization | <ul style="list-style-type: none"> • Weak mechanical properties • Limited selection of polymers and reinforcement |
| Ceramics | <ul style="list-style-type: none"> • Aerospace • Automotive • Chemical Industries • Biomedical | <ul style="list-style-type: none"> • Porosity of lattices controlled • Reduced fabrication time • Composition and | <ul style="list-style-type: none"> • Limited choice of 3-D printing ceramics • Improper dimension • Improper surface finish |

| | | | |
|----------|--|---|--|
| | | microstructure are controlled. | |
| Concrete | <ul style="list-style-type: none"> • Infrastructure • Construction | <ul style="list-style-type: none"> • Huge customization • Less labor required | <ul style="list-style-type: none"> • Layer by layer appearance • Anisotropic mechanical property |

1.6. Application and challenges

Table 4 Additive manufacturing process types with applications

| Prototypes | Casting patterns & Cores | Manufacture tools, jigs & fixtures | Manufacture blanks | Manufacturing end-user loaded parts | Repair of part |
|--------------------------|--------------------------|------------------------------------|--------------------|-------------------------------------|----------------|
| 15 Sheet lamination | | | | | |
| Binder Jetting | | | | | |
| Material Jetting | | | | | |
| Vat photo polymerization | | | | | |

| | | | |
|--------------------|--|--------------------------|--|
| Material Extrusion | | | |
| Powder bed fusion | | | |
| | | Direct energy deposition | |

The drastic and quick changes in the customer requirement can be fulfilled in industries like automobiles and aerospace by utilizing AM technology. This technology has shaped the direction and develop technological innovations that help the companies to meet with the demands of the market. AM is the biggest innovation as it opens the new scope in the companies and provides many possibilities to improve manufacturing efficiency. The main sector which used 3-D printing are:

❖ **Aerospace industry**

In the aerospace industry, titanium and nickel alloys are used to make a lightweight device. The main factors these days that need to be considered in the aerospace industry are weight and fuel saving. This can be effectively done using additive manufacturing technology.

❖ **Medical and dental industry**

In the medical and dental industry, for fabricating orthopedic or orthodontic implants titanium alloys have been extensively used in the form of powder. Mass customization at an affordable price is the main driving factor for implementing additive manufacturing in this industry.

❖ **Automotive**

The Automotive sector largely depends on additive manufacturing technology. This sector is the second largest sector that produces products by additive technology. Design flexibility is the major factor that leads to an increased used of additive manufacturing in this sector. Apart from design flexibility, rapid prototyping is another factor that plays role of using additive manufacturing in this sector.

❖ **Consumer Products**

This is the largest sector that used additive manufacturing to produce products. Apart from the largest, this sector is the most diverse sector that produces a large range of products by embracing additive manufacturing technology. The high level of customization is the main factor that leads to use this technology in this sector.

❖ **Construction**

Most of the work of additive manufacturing in the construction industry works around the extrusion process of materials using aggregate-based material for a high level of application. The use of polymers as a material has been effective for aesthetic purposes that have unique designs.

❖ **Food Industry**

The benefits of 3-D printing are various in food industry. It helps in fabricating complex designs that are required in the machinery of food industry. It helps in calibrating the tools of food industry.

❖ **Education Industry**

Additive manufacturing has made learning process much easier at all the level i.e. primary level to university level. It helps students to print design the components much easily as compare to other outside sources.

Table 5 Application of 3-D printing

| INDUSTRY | APPLICATION |
|---|--|
| <p>AEROSPACE</p> <p>1.Design & rapid prototyping</p> <p>2. Component Manufacture</p> <p>3.Mass customization</p> | <p>1. Light weight of aircraft</p> <p>2. Engine components</p> <p>3. Flight-certified hardware</p> <p>4.Airplane landing gear assemblies</p> |
| <p>MEDICAL</p> <p>1.Design and rapid prototyping</p> <p>2. Manufacture at requirement</p> <p>3.Mass customization</p> | <p>1. Manufacture human organs 2. Reconstructing bones, body parts</p> |

| | |
|---|--|
| <p>AUTOMOTIVE</p> <ol style="list-style-type: none"> 1. Simplify production process 2. Component Manufacture 3. Design &Rapid prototyping 4. Manufacture at requirement | <ol style="list-style-type: none"> 1.Light weight 2.Cooling system for racing cars 3.BMW is using print hand tools 4. <p>Can be used in a backup capacity</p> |
| <p>ARCHITECTURE & CONSTRUCTION</p> <ol style="list-style-type: none"> 1.Design & rapid prototyping 2. Manufacture at requirement | <ol style="list-style-type: none"> 1.Design & rapid prototyping 2. Manufacture at requirement |

1.7. Fused Deposition Modelling

Fused Deposition Modelling (FDM) is one of the most widely used consumer focused additive manufacturing technology. FDM is relatively easier to setup and use as compared to other additive manufacturing technologies available to consumers today. Also, it is much more economical to operate than its counterparts in the domain. FDM technology is usually seen in desktop 3D printers so that an individual can easily and rapidly visualize the design physically, check the functionality and prepare a prototype of any idea.

FDM uses polymers as its raw materials. The most widely used polymers in this technique is Acrylonitrile Butadiene Styrene (ABS), Poly Lactic Acid (PLA) and Nylon. The materials used to make a 3D prints in the FDM environment, have a considerably low mechanical strength which limits its usage to desktop printers. In FDM, a thin filament of wire is extruded in a semi molten state, through a nozzle and is deposited on the build platform. The process of making a prototype starts from a Computer Aided Design (CAD) data. The CAD data is then converted into Standard Tessellation Language (STL) file. A STL file only represents the surface of the CAD Model with a mesh of triangles composed of vertices edges and faces. The size of the triangle is refined to capture the fine details present in the CAD design. The STL data is then divided into layers using software or open source codes. The dividing of STL data into layers is known as slicing i.e. the surface is divided into finite number of layers. The process parameters, which influence the final quality of the prototype starts from the slicing process. Any sliced layer represents the perimeter of a cross section of the solid model or CAD model. The perimeter generated after slicing defines

the work domain of the printing. After slicing, the desired print quality is examined and the process parameters or the printer settings are calibrated in the virtual an environment or hardware of the machine itself.

1.8. Process Parameters

Fused Deposition Modelling machines have a wide range of processing parameters. The quality of the workpiece is a function of combination of the following parameters.

1. **Layer height** is the minimum thickness of a layer that is stacked together to generate height for the workpiece. Reduced layer height results in highly detailed workpiece and consumes a considerable amount of time whereas, increased layer height skips geometric details which have dimensions less than the layer thickness. One of the widely practiced ways to achieve quality in less time is employing “Adaptive Slicing”. In adaptive slicing height of layers are distributed throughout the thickness of the CAD model as a function of geometric details present in the model. Layer height is reduced in volumes where the fine details are needed and increased where the details are absent to save time. By doing so the quality of the print is affected.
2. **Initial layer height** is the thickness of the first layer deposited on the build surface. Making a perfect first layer is the cornerstone for making a high-quality part. Getting the first layer right requires low travel speed, right air gap between the nozzle & build surface, adhesion of first layer with the build surface and an increased layer height. A perfect first layer keeps the entire job firmly attached to the build surface which is very important to achieve quality.
3. **Line width** affects cross sectional area of the extruded wire or overlap of the adjacent filaments. Usually width of filament is diameter of the printing nozzle. Slightly reduced line width produces a clean print with acceptable quality and lower value of the line width generates voids in layers.
4. **Wall thickness** refers to the thickness of side walls or the perimeter of the layer. It is specified by numerically defining the thickness or the number of lines in the wall. Wall constitutes of thin extruded filaments as lines laid down adjacent to each other.
5. **Top / Bottom thickness** is thickness of the top and bottom surface. Like wall thickness it is defined as a numerical value or as several layers. Together combining these parameters, wall thickness and top / bottom thickness creates a shell of a specific thickness. Shell provides an

appearance of a complete solid and imparts additional strength. Top and bottom surface of the shell is a layer, it has a specific design of infill which is customizable as per the requirement from the surface.

6. **Infill** is a structure which occupies the volume inside of a shell. The only function of an infill is to provide internal structural support to the part and act as a load bearing and transferring element. To define an infill, two parameters are most important. One is the type of infill i.e. cross diamonds, honeycomb etc. and other is density of the infill type. Type and density of infill ²¹ plays a very crucial role in characterizing the mechanical strength of the part. Density of infill is controlled by defining size of an individual element.
7. **Printing / Nozzle temperature** ³⁰ is the temperature at which raw material is extruded out of the nozzle. It controls the viscos elastic behavior of the filament. The filaments are fused together thermally to form a solid joint. However there exists a finite temperature gradient throughout a layer which affects the thermal fusion process. High temperature extrusion generates more window for the thermal fusion, but a slight compromise is also achieved in the dimensional accuracy. Increasing the temperature ensures the semi molten material flows more freely and fills the voids that are formed during the extrusion and fusion process.
8. **Build plate temperature**, is temperature of the first layer in contact with the build surface. Higher build temperature is necessary for good adhesion with build surface. Another parameter which is also responsible for build plate adhesion is build plate temperature.
9. **Print speed**, controls motion of nozzle throughout the build surface. Varying print speed affects thermal fusion of the layers.

Many FDM machine manufactures have a standard combination of these factors to produce quality products. However, the standard settings are not suitable for every design fed into the machine. A deeper study of combination of factors and its influence on overall property of the workpiece is necessary to achieve printed products of desired quality. The greatest advantage additive manufacturing has over other manufacturing technologies is its tremendous capability to tackle most complex geometries. To get a part manufactured accurately in a first attempt requires a clear understanding of the parameters. A set of parameters might show exceptional results for a product, but the same set of parameters might also make another product inclined towards premature failure. Externally, a part produced through additive manufacturing may look completely identical to several other parts designed for same functionality, but their internal load bearing structures can be

completely altered. The configuration of an internal load bearing structure is controlled by a combination of process parameter employed by a user. The reason behind such a changed behavior is the response of the internal structural elements of the product.

CHAPTER 2

LITERATURE REVIEW

This chapter provides a quick overview of current developments in the field of additive manufacturing. AM is a material-adding technique in which one layer of material is laid down on top of another. In most classical manufacturing processes, the part is created through subtraction and machining. The fused deposition modelling process is the most frequently utilized and cost-effective AM approach.

A brief literature review has been conducted in this chapter on several aspects of the AM process, particularly in the field of fused deposition modelling. The research was done on the fabrication side to see how processing parameters in the FD[1]M process affected the outcome.

1. According to Li Yi et al. (2017)[1], 3-D Printing is the umbrella word for manufacturing activities which involve layer by layer material addition to form parts. Rapid prototyping, tooling, and direct manufacturing of functional parts, all of which have revolutionary effects on the manufacturing business. It covers four aspects of AM technologies: primary hurdles to AM technology, total cost of AM application estimation, design of hybrid additive-subtractive process chains, and quality management with AM.
2. Tuan D.Ngoa et al (2018)[2] studied the current state of AM technology, as well as the materials and procedures used in AM technology. Metal alloys, polymer, composites, ceramics, and concrete are some of the key materials used in AM technology.
3. SM Fijul kabir et al. (2019)[3] discussed the historical background of Additive manufacturing. He proposed CFF composites to serve for high load.

4. Kathrin Pfahler et al. (2019)[4] has highlighted how ²² companies have started to use AM across the product cycle, from prototype development to final product sale to customers. The results of his research revealed AM's current and future applications.
5. K.Rajaguru et al. (2019)[5] have conducted research on ⁹ additive manufacturing techniques, digital pre-processing procedures integration, and product-based process design. The process of developing new models has also been examined to shorten development and manufacturing time.
6. Ugur M Dilberoglu et al. [6] has focused on ¹⁸ the role of additive manufacturing in the era of industry 4.0. He reviewed the contribution of additive manufacturing to industry 4.0.
7. Daniel Delgado Camacho et al[7]. has talked about how additive manufacturing can be used in the construction business. He mentioned the different processes and potential application of additive manufacturing in the construction business. He also discussed about the materials that can be employed in the field of building when it comes to additive manufacturing.
8. Mohd javaid et al.[8] take the case of dentistry, where he examined the applicability and benefits of AM in dentistry, as well as the methods involved in creating a 3-D printed dental model. In the case study, additive manufacturing technology is utilized to create complicated dental crowns, bridges, and orthodontic braces, as well as other models, equipment, and instruments in less time and at a lower cost.
9. R.J Zaldivar and D.B Witkin[9] reviewed that the build orientation direction affects mechanical properties including tensile strength, failure strain, modulus, and poisson's ratio. In comparison to injection mold parts, the strength of FDM parts rose from 46 to 85 percent when the build orientation direction of printing was optimized.
10. Ertan G[10] provides an overview of biocarbon polymer materials that can be used in 3D printing. PLA (Polylactic acid) is a biopolymer substance that is used in 3D printing for a variety of applications, including house structures, consumer products, physical prototypes, and vehicle interior parts, among others. PLA is a biodegradable substance that can be used to improve soil quality. The author presents a quick overview of the structural and tribological features of PLA filaments that are commonly used in 3D printing. The author concluded that scanning electron microscopy (SEM) can identify good bonding between bio carbon reinforcement and PLA material, and that the interfacial bonding strength may be validated in future studies.

11. Williams RE et al.[11] studied that the first rapid prototyping method was stereolithography. Design conceptualization, medical modelling, biomedical implants, and quick tooling are all characteristics of this procedure. For dimensional precision, this method offers a variety of print types. They discovered that layer resolution is one of the most important factors influencing part strength.
12. Dietmar Frank et al.[12] studied that parts are manufactured using a layered manufacturing method. In the layered manufacturing process, the build orientation direction is critical for improving the part's quality and shape. Because it minimizes production build time, increases support structure, quality, design, and manufacturing cost, build orientation is regarded a significant characteristic in the manufacturing business. The current study makes use of an expert tool system that considers a variety of factors that influence prototype construction.
13. A K Sood and R K Ohdar[13] explained that many factors influence the dimensional accuracy of FDM parts. They investigated five parameters, namely part build orientation, layer thickness, raster width, raster angle, and air gap, interacted with the Taguchi L27 orthogonal array. They concluded from the experimental data that the measured dimension is always greater than the required value along the thickness direction, while the diameter of the hole, length, and width of the test portion are all less than the desired value. They used the grey Taguchi approach and discovered certain optimum factors. The overall dimensional correctness of FDM manufactured pieces ²³ is predicted using an artificial neural network (ANN).
14. Randall S. Sexton[14] explained that a neural network is a technique that can be used to approximate an unknown variable ²⁶ to any degree of precision. Back propagation is the greatest optimization approach for neural network training and testing. The author examines the performance of two global search techniques: Genetic Algorithm and Simulated Annealing.
15. Carsten Koch et al.[15] By modifying parameters like bead orientation, layer height, and solidity ratio, we were able to reach tensile strengths that were very near to injection molded specimens. Various open source software, such as SciSlice, can be used to create a customized layer. The orientation of load-carrying fibers is referred to as bead orientation. When compared to any other orientation, fibre oriented along the direction of load bear the most stress. When you lay down filaments in a layer, voids are necessarily present. The authors devised a statistic called the solidity ratio to measure these voids. There are fewer voids when the solidity ratio is higher. The volumetric flow rate of the nozzle or the distance between two neighboring filaments can be used

to modify the solidity ratio. High SR also creates a larger welding area between the filaments, resulting in higher molecular diffusion and strength.

16. Jun Yin et al.[16] through the research, have investigated the effects of process factors on interfacial bonding strength. The nozzle temperature, build bed temperature, and printing speed were the process variables that were considered. The strength of bonding at the interface of two different materials is measured using the multi-material FDM model. Their findings show a 93 percent increase in bonding strength between Thermoplastic Polyurethane (TPU) and Acrylonitrile Butadiene Styrene at an interface (ABS). The roughly doubling of the building bed temperature is responsible for the observed increase in bond strength. The observed influence of nozzle temperature, on the other hand, only contributed around 15% to the binding strength at the contact.
17. Jianlei wang et al.[17] consider modifying the raw material used for printing instead of tweaking the process settings to improve mechanical qualities. To improve mechanical qualities, thermally expandable microspheres were combined with poly wax powder and filaments. The influence of high temperatures on the mechanical strength of the manufactured samples employing modified filaments was noticed. There was a favorable impact on mechanical properties. The tensile and compressive strength of materials heated at 140°C for 120 seconds with 2 wt. percent microspheres rose by 25.4 percent and 52.2 percent, respectively.
18. Chamil Abeykoon[18] conducted an experimental study focusing on mechanical, thermal, and morphological for PLA, ABS, CFR PLA, CFR ABS and CNT ABS specimens. The process parameters included are infill density, infill speed, infill pattern and printing temperature. Young's modulus for pure PLA, increase as we increase infill density While young's modulus first increase then decrease with increase in infill speed. With increase in temperature of nozzle up to 205°C tensile modulus decreases then up to 215° C increase.
19. Mst Faujiya Afrose[19] investigated experimentally the effect of build orientation on tensile properties of PLA and found parts printed along x axis (built direction) have maximum tensile strength followed by 45° then y axis.
20. M. Kamaal[20] investigated the tensile strength and impact strength of carbon fiber PLA composite. By considering 3 process parameters i.e. build direction, infill percentage and layer height. It was found to be with increase in infill percentage and layer height tensile strength

increase while in case of impact strength, it increases with increase in infill percentage and decrease with layer height

21. Farhad Mohammad Othman[21] investigated the influence of infill density, layer thickness, part orientation on UTS of FDM printed PLA parts and it was found that infill density contributed to 35 % followed by layer thickness (33%) and printing orientation. It was found that with increase in layer thickness and infill percentage tensile strength increase. He also investigated their influence on compressive strength and bending strength.
22. Rachit Omer[22] investigated the tensile performance for Short carbon fibre PLA composites He considered layer thickness, infill percentage and layer position and their interactions It was found that with increase in layer thickness and infill percentage ,tensile strength increase but with layer position , tensile strength decrease. He future created neural network for optimization and prediction
23. Shilpesh R. Rajpurohit[23] through his research, investigated the effect of raster angle, layer thickness and raster width on PLA. It was found experimentally highest tensile strength is obtain with 0° raster angle. However, with increase in layer thickness, tensile strength decrease. Also, at higher value of raster width tensile strength is improved up to certain strength.
24. Xinzhou Zhang[24] investigated the effect of raster angle on mechanical properties of PLA specimen and it was found experimentally that with increase in raster angle from 0 to 90 tensile strength decrease
25. V. Durga Prasada Rao[25] in his work investigated the effect of print temperature, layer thickness and infill pattern for PLA specimen With increase in temperature from 205°C to 225°C, tensile strength is increased .out of cubic, cubic sub division and quarter cubic infill pattern, specimen with cubic infill pattern show maximum tensile strength.
26. R. Srinivasan[26] through his research investigated the effect of infill pattern .in his study he investigated the influence of different infill patternlike triangular, grid, cubic, honey comb, concentric, rectilinear, rectangular, octet and wiggle and found that tensile strength of grid is maximum among all infill pattern for PLA specimen.

CHAPTER 3

MODELLING AND FABRICATION OF TEST SPECIMENS

3.1. Modeling

There exist no well-defined rules, on how to manufacture a tensile test component through additive manufacturing. This adds freedom to experiment with the design and manufacturing capabilities achievable for additive manufacturing technologies. To fabricate a tensile test specimen made up of plastic, ASTM D638 testing standard was used as a reference document to establish the dimensions of the specimen. The CAD geometry for the specimen was developed in Autodesk Fusion 360. The dimensions shown in figure 4 are in millimeters. The thickness of this flat specimen was taken as 3.20 mm. As shown in figure 4 The modelled test specimen was flat dumbbell shaped CAD model. Now the next step towards fabrication is, converting this CAD data into a STL data. Converting is a simple step and is easily done in the Solidworks 2020. The CAD data can be directly saved as a STL file in Fusion 360. Figure 4 shows the STL file preview of the CAD data. The CAD data is represented as a surface consisting of triangles.

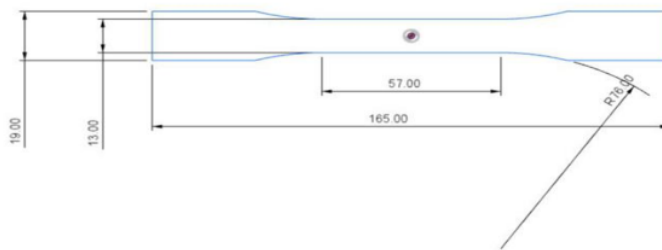


Figure 4 Dimensions of Tensile Test Specimen

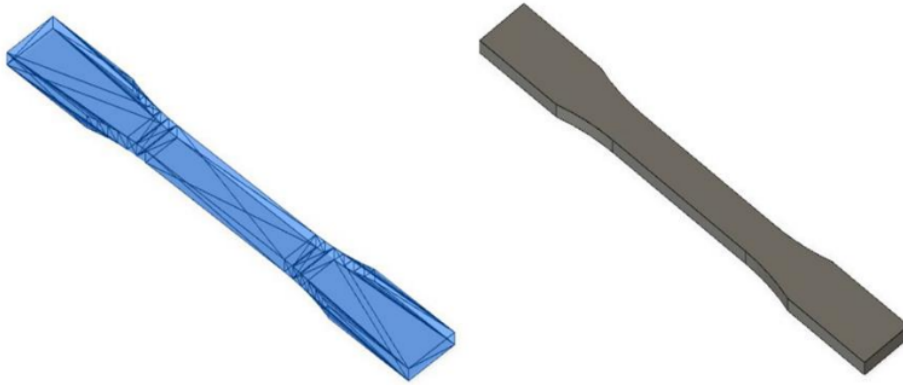


Figure 5 STL and CAD model of Tensile Test Specimen

The refinement option of the triangles was kept at high, so that the details and curvature of the design are captured. STL file is then loaded in a slicing software, where two dimensional cross sections are generated from the surface body. The above stated two-dimensional cross section is essentially a perimeter for any cross section of the CAD data. The perimeter helps in identifying a working domain for the 3D printer.

3.2. Selection of Process Parameters

To obtain a profound set of results Taguchi's Design of Experiment philosophy was used to design statistical set of experiments. In this philosophy values of a parameter or parameters are changed in a systematic manner to observe the response of desired output. Fusebot 250+ has an approximate build volume of 52 cm x 44 cm x 65 cm, which large enough to try out various orientations for a product.

One of the major reasons behind poor mechanical behavior of FDM printed parts is, the presence of voids and other is the bonding within layers as well as in between the layers. Voids and imperfectly bonded filaments make the final printed part highly anisotropic in nature.

The Fusebot 250+ printer can print high-resolution layers with thicknesses of 100, 150, and 200 micrometers per layer. High-resolution printer settings lay down a fiber extremely close to it, which minimizes the size of voids significantly, but it takes a long time to print. The second parameter is the printing temperature of PLA material ranging from 190° C to 210° C. The type of plastic used in 3-D printing is determined by the temperature at which it is printed. More welding time and better bonding development at the interface are possible with high-temperature component printing.

However, exceeding the recrystallization temperature by a significant amount can result in uneven workpiece printing. Different printing speed are used ranging from 40 mm/s to 70 mm/s in a step of 10 mm/s. Higher the printing speed, lesser the printing time. Fusebot 250+ can print up to 200mm/s. Fourth factor that is considered is Infill pattern and last factor is taken as raster orientation.

3.3. Orthogonal array

Taguchi design is an excellent strategy for selecting unique arrangements of combinations termed orthogonal arrays, rather than completing all feasible combinations. The control parameters and selected settings are used to construct an appropriate Taguchi OA. The number of factors and the levels for each component influence the choice of an OA. MINITAB V19 creates an L27 orthogonal array with the assumption that there is no interaction between the selected factors. The parameters' values are presented in Table 6.

Table 6 Taguchi L27 Orthogonal Array

| layer thickness | nozzle temperature | Speed/feed rate | structure | Raster orientation |
|-----------------|--------------------|-----------------|----------------|--------------------|
| 100 | 190 | 40 | rectilinear | 0 |
| 100 | 190 | 40 | rectilinear | 45 |
| 100 | 190 | 40 | rectilinear | 90 |
| 100 | 200 | 50 | full_honeycomb | 0 |
| 100 | 200 | 50 | full_honeycomb | 45 |
| 100 | 200 | 50 | full_honeycomb | 90 |
| 100 | 210 | 60 | grid | 0 |
| 100 | 210 | 60 | grid | 45 |
| 100 | 210 | 60 | grid | 90 |
| 150 | 190 | 50 | grid | 0 |
| 150 | 190 | 50 | grid | 45 |
| 150 | 190 | 50 | grid | 90 |
| 150 | 200 | 60 | rectilinear | 0 |
| 150 | 200 | 60 | rectilinear | 45 |
| 150 | 200 | 60 | rectilinear | 90 |
| 150 | 210 | 40 | full_honeycomb | 0 |
| 150 | 210 | 40 | full_honeycomb | 45 |

| | | | | |
|-----|-----|----|----------------|----|
| 150 | 210 | 40 | full_honeycomb | 90 |
| 200 | 190 | 60 | full_honeycomb | 0 |
| 200 | 190 | 60 | full_honeycomb | 45 |
| 200 | 190 | 60 | full_honeycomb | 90 |
| 200 | 200 | 40 | grid | 0 |
| 200 | 200 | 40 | grid | 45 |
| 200 | 200 | 40 | grid | 90 |
| 200 | 210 | 50 | rectilinear | 0 |
| 200 | 210 | 50 | rectilinear | 45 |
| 200 | 210 | 50 | rectilinear | 90 |

3.4. Fabrication and Experimental Setup

The 27 samples are printed according to the Taguchi L27 orthogonal array are shown in Figure 8. The specimens were printed on a Fusebot 250+ printer. The electromechanical universal testing machine is utilized to test the tensile strength of PLA material. The fabricated components were tested using computerized tensile testing machine (TKG-EC-50). TKG-EC-50 has a servo drive mechanism to pull grips and apply strain, with a range of 0.2 – 500 mm/min. For testing, strain rate of 3 mm/min used to apply loads. The machine has a maximum load cell value of 50KN. Loading accuracy is with $\pm 1\%$. Figure 7 shows the experimental setup



Figure 6 Fusebot 250+



Figure 7 TKG EC 50



Figure 8 Fabricated Samples

3.5. Artificial Neural Network

The artificial neural network (ANN) originally developed out of a fascination with the human brain's

capabilities as a computational tool in the 1940s. It is now one of the most used computational tools in the world. The human brain is extremely capable of learning, adapting, and evolving. ANN works in a similar manner. ANN is made up of artificial neurons that are connected in a complicated way to map inputs and outputs. The creation of layers with neurons is the preliminary step in creating a neural network. The neurons in one layer are linked to neurons in another layer. To process inputs, each of these connections and neurons is given weights and biases. Furthermore, in the ANN model, 70% of the data is used for training [27, 28], with the remaining 30% being used for testing. The tangent sigmoid activation function was used in this investigation, and a feed-forward back propagation network was developed for each layer. In this study, ANN is used as a prediction tool to check the tensile strength value at the best parameter setting. It is an iterative procedure to work with ANN.

CHAPTER 4

TESTING AND EXPERIMENTAL SETUP



Figure 9 Experimental setup during and after test

The specimens were manufactured with FFF 3-D printing and tested for tensile strength on a computerized universal testing machine (UTM). The electromechanical universal testing machine is utilized to test the tensile strength of PLA material. The fabricated components were tested using computerized tensile testing machine (TKG-EC-50). TKG-EC-50 has a servo drive mechanism to pull grips and apply strain, with a range of 0.2 – 500 mm/min. For testing, strain rate of 3 mm/min used to apply loads. The machine has a maximum load cell value of 50KN. Loading accuracy is with $\pm 1\%$. Figure 9 shows the experimental setup

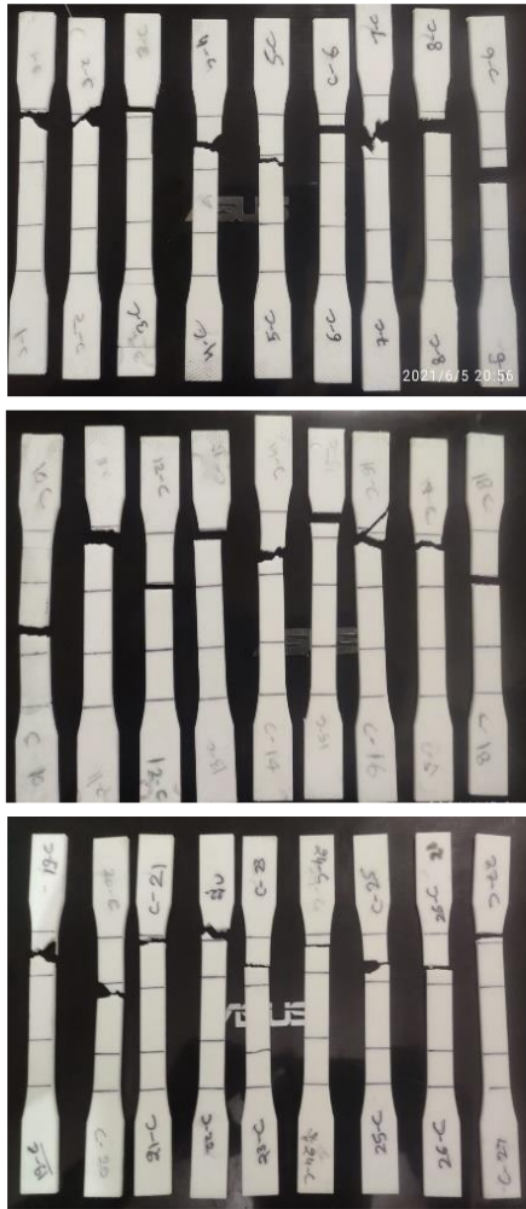
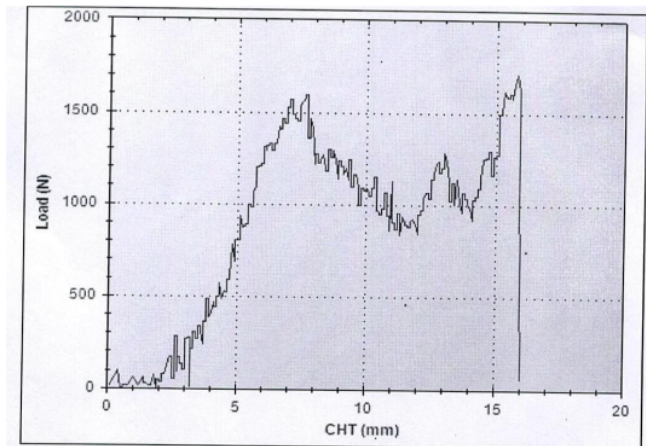
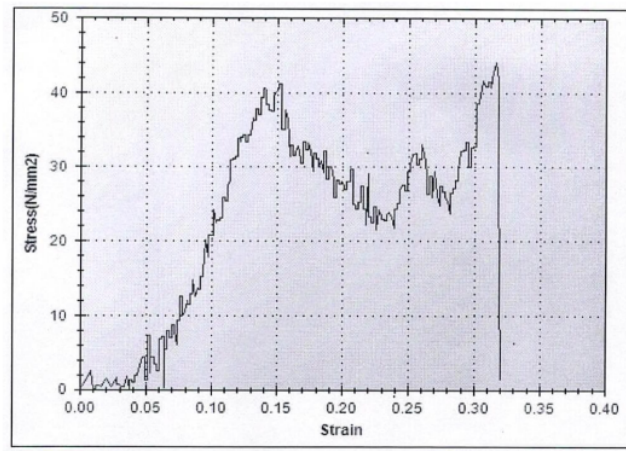


Figure 10 Sample after testing

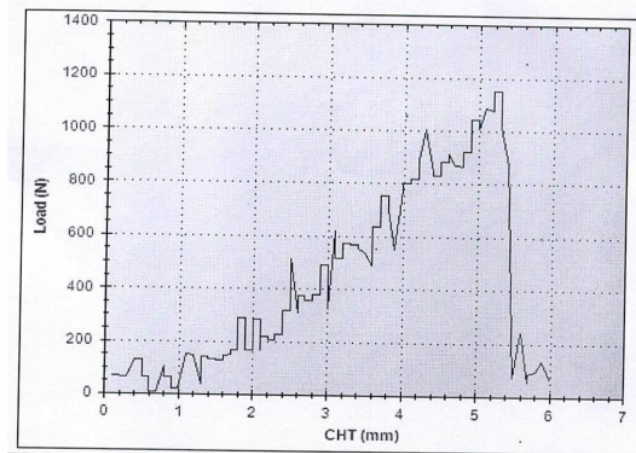


Graph 1 Experimental load-¹ displacement graph of sample 1

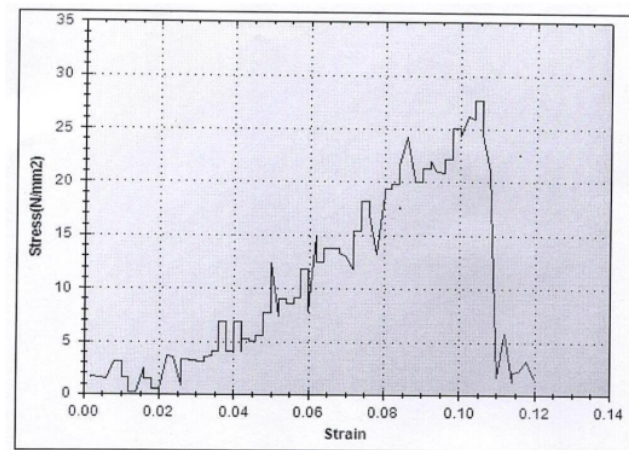


Graph 2 Experimental Stress- Strain graph of sample 1

| Gauge Length (in mm) | Final Gauge Length (in mm) | Peak Load (in N) | UTS (in MPa) | %age Elongation |
|----------------------|----------------------------|------------------|--------------|-----------------|
| 50 | 51.13 | 1710 | 44.118 | 2.26 |

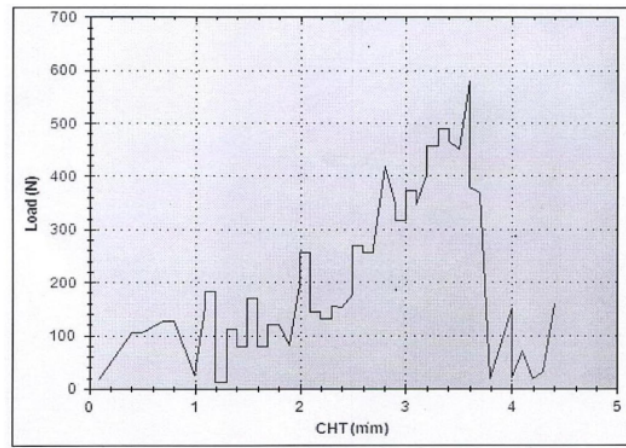


Graph 3 Experimental load-¹ displacement graph of sample 2

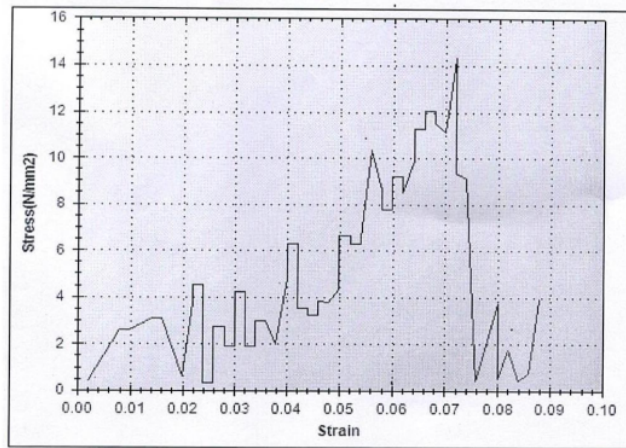


Graph 4 Experimental Stress- Strain graph of sample 2

| Gauge Length (in mm) | Final Gauge Length (in mm) | Peak Load (in N) | UTS (in MPa) | %age Elongation |
|----------------------|----------------------------|------------------|--------------|-----------------|
| 50 | 51.06 | 11475 | 27.69 | 2.12 |

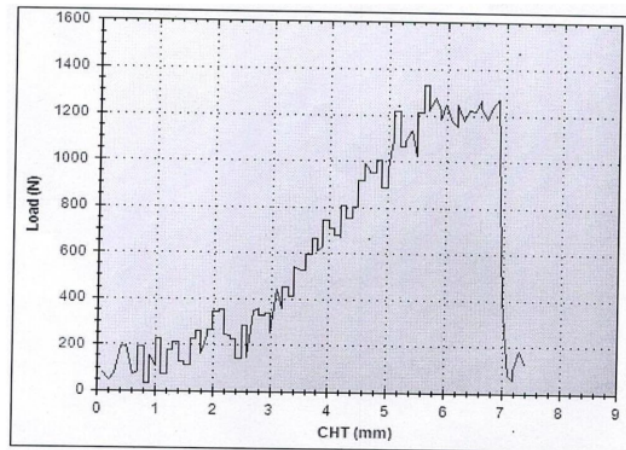


Graph 5 Experimental load-¹ displacement graph of sample 3

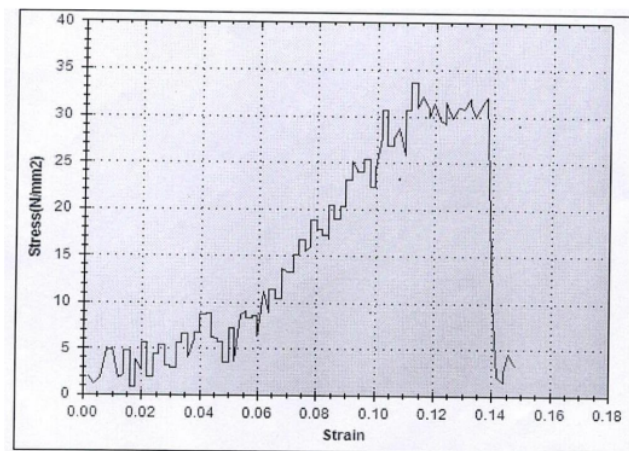


Graph 6 Experimental Stress- Strain graph of sample 3

| Gauge Length (in mm) | Final Gauge Length (in mm) | Peak Load (in N) | UTS (in MPa) | %age Elongation |
|----------------------|----------------------------|------------------|--------------|-----------------|
| 50 | 50.34 | 580 | 14.32 | .68 |

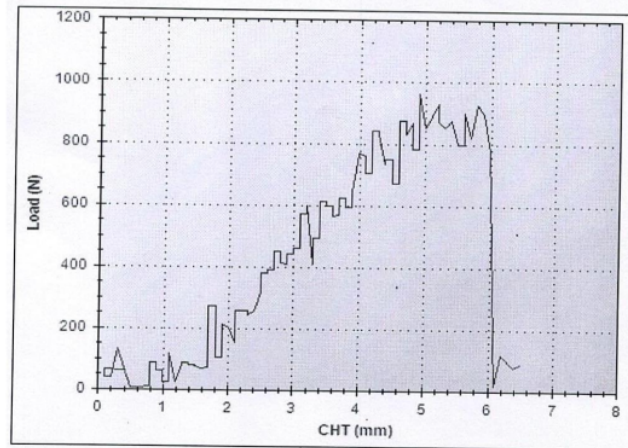


Graph 7 Experimental load- displacement graph of sample 4

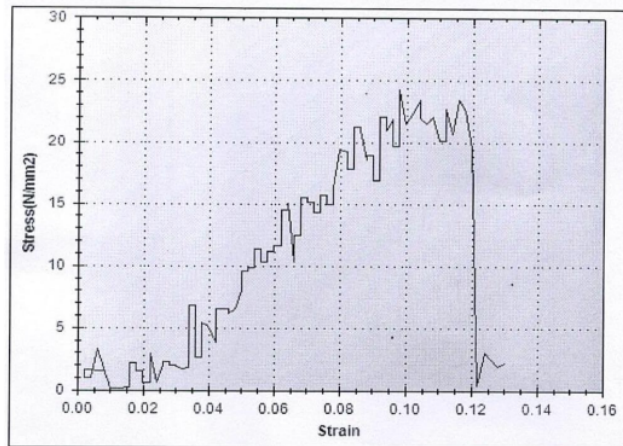


Graph 8 Experimental Stress- Strain graph of sample 4

| Gauge Length (in mm) | Final Gauge Length (in mm) | Peak Load (in N) | UTS (in MPa) | %age Elongation |
|----------------------|----------------------------|------------------|--------------|-----------------|
| 50 | 51.07 | 1330 | 33.605 | 2.14 |

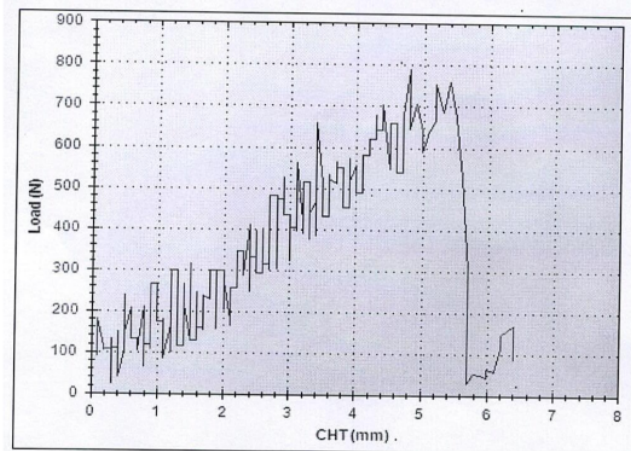


Graph 9 Experimental load-¹ displacement graph of sample 5

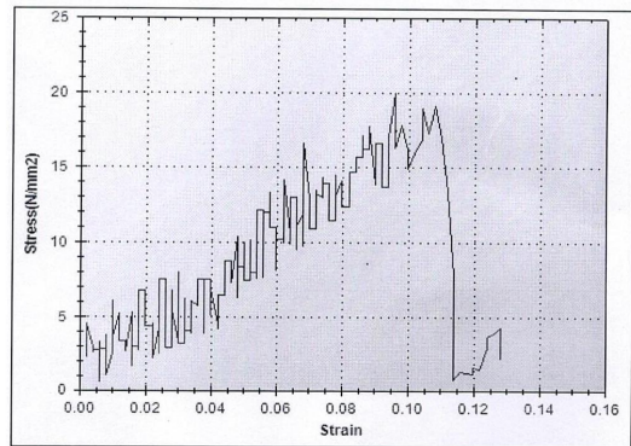


Graph 10 Experimental Stress- Strain graph of sample 5

| Gauge Length (in mm) | Final Gauge Length (in mm) | Peak Load (in N) | UTS (in MPa) | %age Elongation |
|----------------------|----------------------------|------------------|--------------|-----------------|
| 50 | 51.22 | 962.5 | 24.278 | 2.44 |

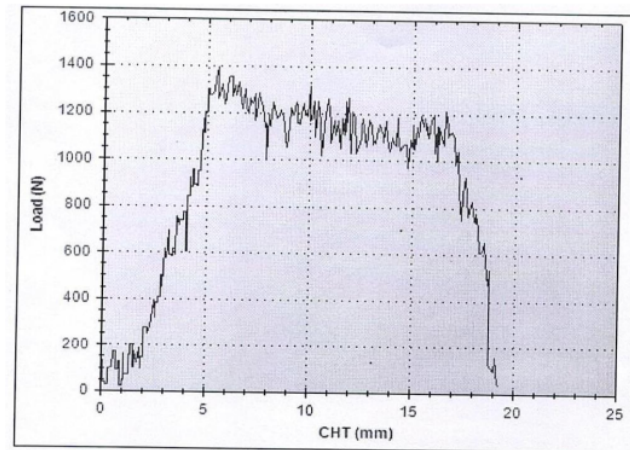


Graph 11 Experimental load-displacement graph of sample 6

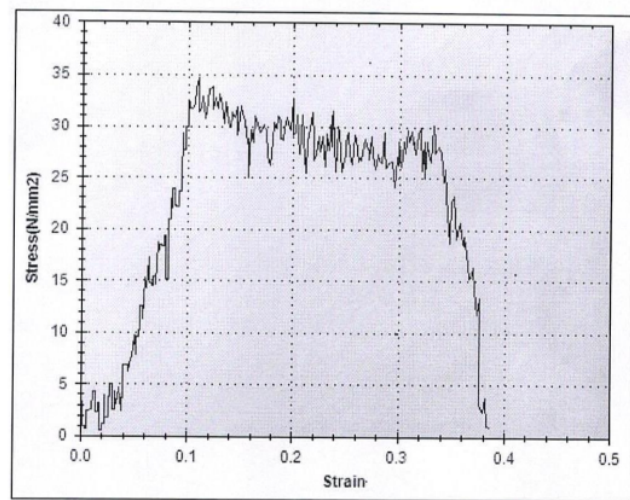


Graph 12 Experimental Stress-Strain graph of sample 6

| Gauge Length (in mm) | Final Gauge Length (in mm) | Peak Load (in N) | UTS (in MPa) | %age Elongation |
|----------------------|----------------------------|------------------|--------------|-----------------|
| 50 | 50.88 | 790 | 19.95 | 1.76 |

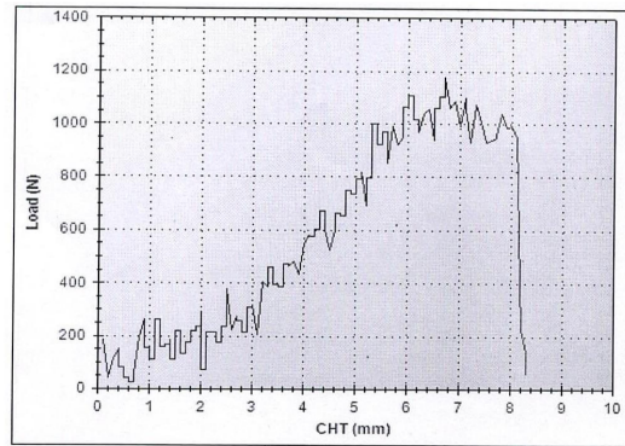


Graph 13 Experimental load- displacement graph of sample 7

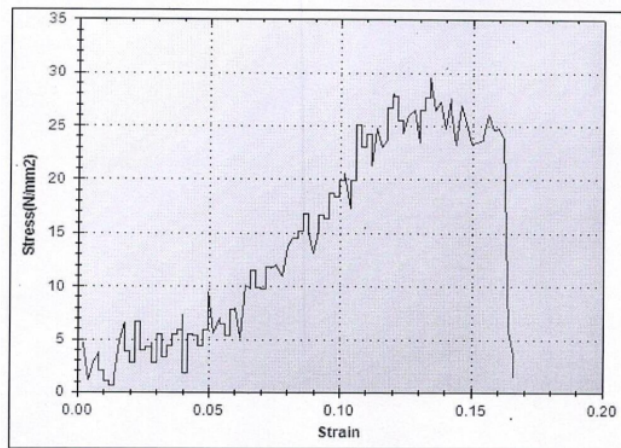


Graph 14 Experimental Stress- Strain graph of sample 7

| Gauge Length (in mm) | Final Gauge Length (in mm) | Peak Load (in N) | UTS (in MPa) | %age Elongation |
|----------------------|----------------------------|------------------|--------------|-----------------|
| 50 | 54.38 | 1390 | 34.637 | 8.76 |

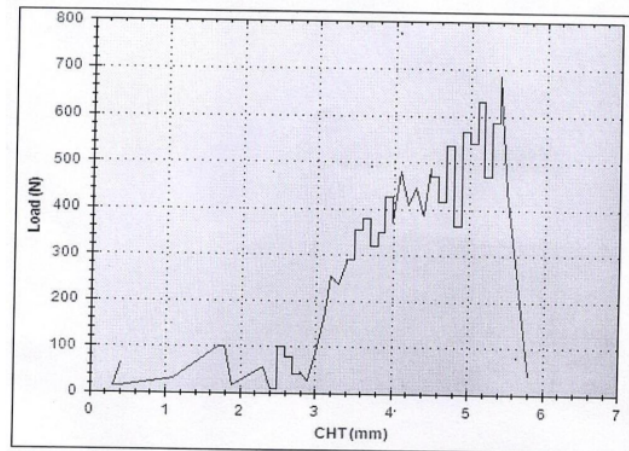


Graph 15 Experimental load- displacement graph of sample 8

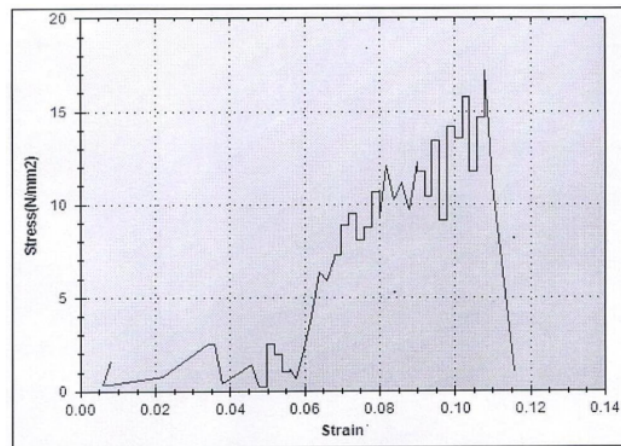


Graph 16 Experimental Stress- Strain graph of sample 8

| Gauge Length (in mm) | Final Gauge Length (in mm) | Peak Load (in N) | UTS (in MPa) | %age Elongation |
|----------------------|----------------------------|------------------|--------------|-----------------|
| 50 | 51.08 | 1175 | 29.44 | 2.16 |

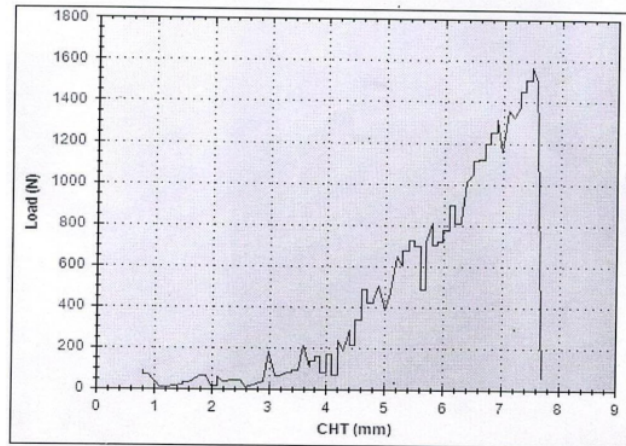


Graph 17 Experimental load- displacement graph of sample 9

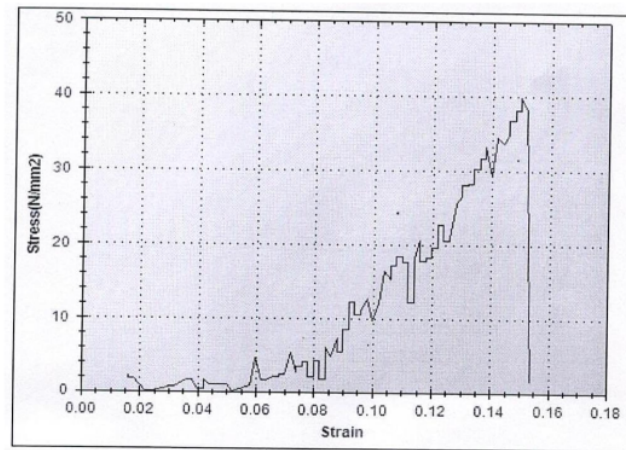


Graph 18 Experimental Stress- Strain graph of sample 9

| Gauge Length (in mm) | Final Gauge Length (in mm) | Peak Load (in N) | UTS (in MPa) | %age Elongation |
|----------------------|----------------------------|------------------|--------------|-----------------|
| 50 | 51 | 685 | 17.143 | 2 |

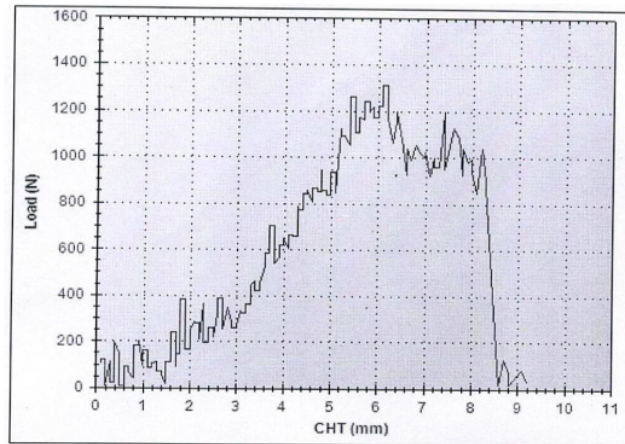


Graph 19 Experimental load- displacement graph of sample 10

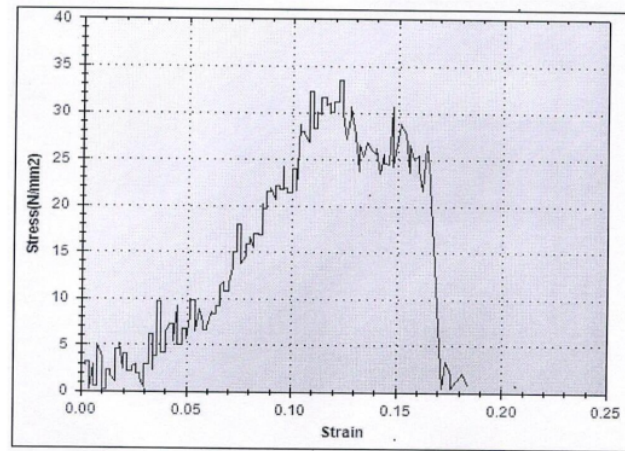


Graph 20 Experimental Stress- Strain graph of sample 10

| Gauge Length (in mm) | Final Gauge Length (in mm) | Peak Load (in N) | UTS (in MPa) | %age Elongation |
|----------------------|----------------------------|------------------|--------------|-----------------|
| 50 | 50.82 | 1567.5 | 39.753 | 1.64 |

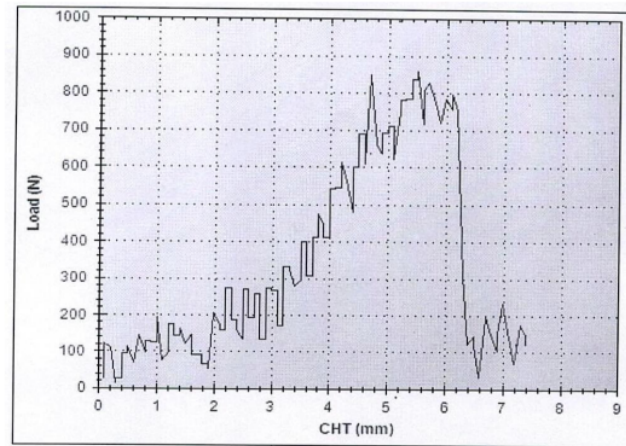


Graph 21 Experimental load- displacement graph of sample 11

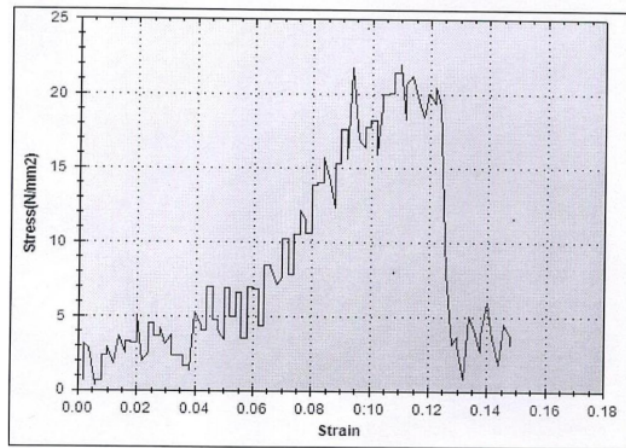


Graph 22 Experimental Stress- Strain graph of sample 11

| Gauge Length (in mm) | Final Gauge Length (in mm) | Peak Load (in N) | UTS (in MPa) | %age Elongation |
|----------------------|----------------------------|------------------|--------------|-----------------|
| 50 | 50.83 | 1310 | 33.496 | 1.66 |

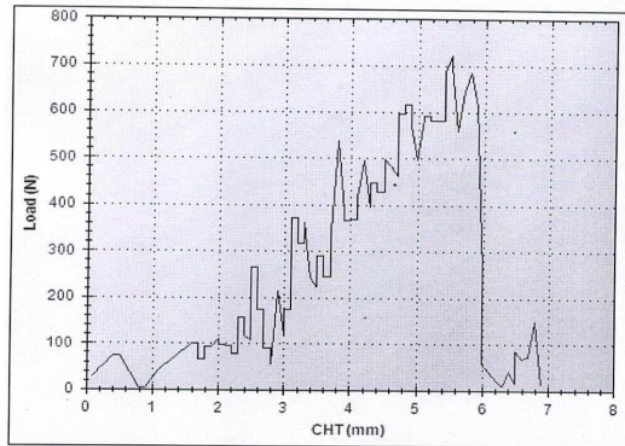


Graph 23 Experimental load- displacement graph of sample 12

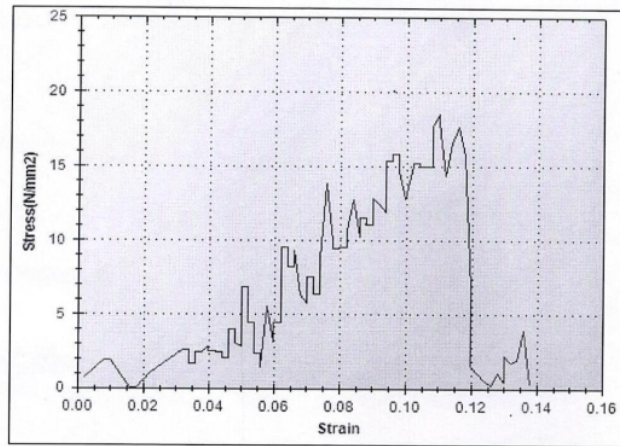


Graph 24 Experimental Stress- Strain graph of sample 12

| Gauge Length (in mm) | Final Gauge Length (in mm) | Peak Load (in N) | UTS (in MPa) | %age Elongation |
|----------------------|----------------------------|------------------|--------------|-----------------|
| 50 | 50.76 | 857.5 | 21.977 | 1.52 |

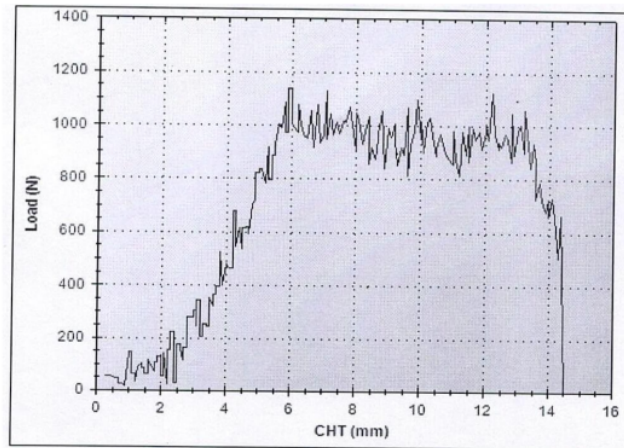


Graph 25 Experimental load- displacement graph of sample 13

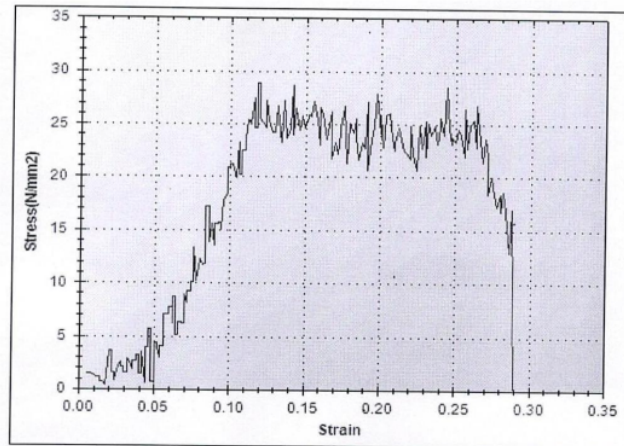


Graph 26 Experimental Stress- Strain graph of sample 13

| Gauge Length (in mm) | Final Gauge Length (in mm) | Peak Load (in N) | UTS (in MPa) | %age Elongation |
|----------------------|----------------------------|------------------|--------------|-----------------|
| 50 | 50.71 | 720 | 18.553 | 1.42 |

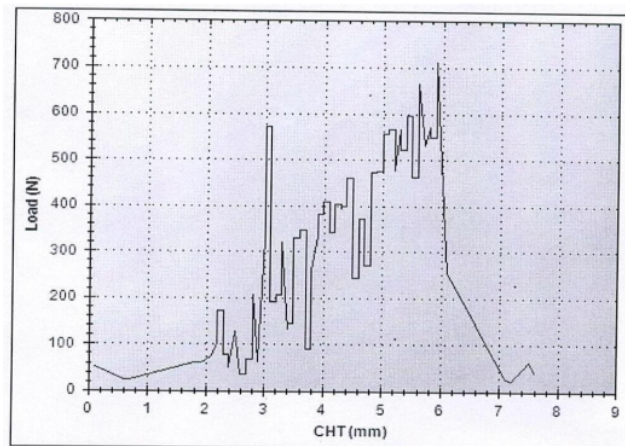


Graph 27 Experimental load- displacement graph of sample 14

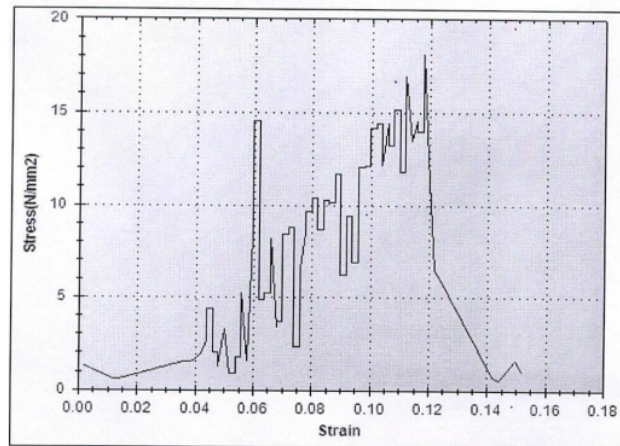


Graph 28 Experimental Stress- Strain graph of sample 14

| Gauge Length (in mm) | Final Gauge Length (in mm) | Peak Load (in N) | UTS (in MPa) | %age Elongation |
|----------------------|----------------------------|------------------|--------------|-----------------|
| 50 | 54.04 | 1135 | 28.79 | 8.08 |

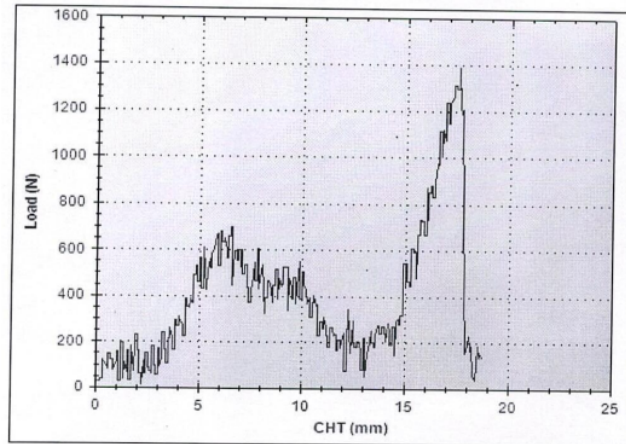


Graph 29 Experimental load-displacement graph of sample 15

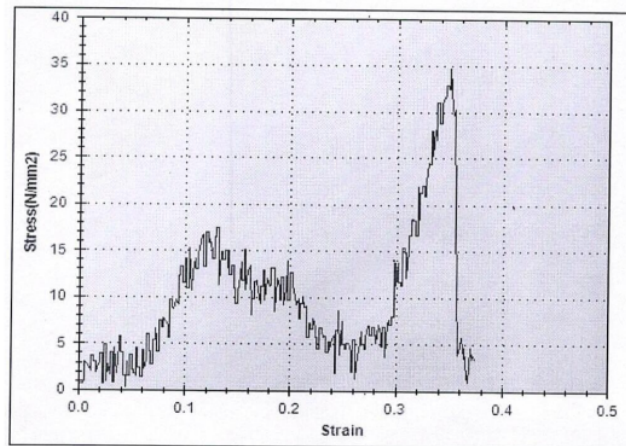


Graph 30 Experimental Stress-Strain graph of sample 15

| Gauge Length (in mm) | Final Gauge Length (in mm) | Peak Load (in N) | UTS (IN MPA) | %age Elongation |
|----------------------|----------------------------|------------------|--------------|-----------------|
| 50 | 50.93 | 710 | 18.061 | 1.86 |

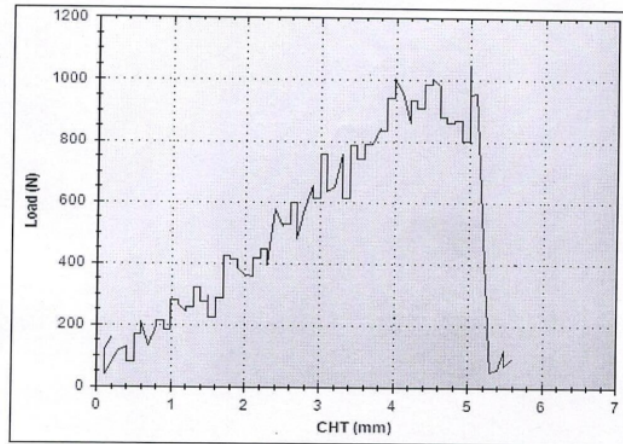


Graph 31 Experimental load- displacement graph of sample 16

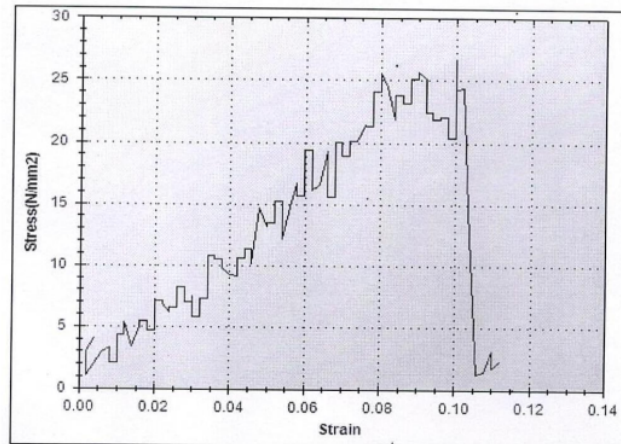


Graph 32 Experimental Stress- Strain graph of sample 16

| Gauge Length (in mm) | Final Gauge Length (in mm) | Peak Load (in N) | UTS (in MPa) | %age Elongation |
|----------------------|----------------------------|------------------|--------------|-----------------|
| 50 | 51.04 | 1385 | 34.741 | 2.08 |

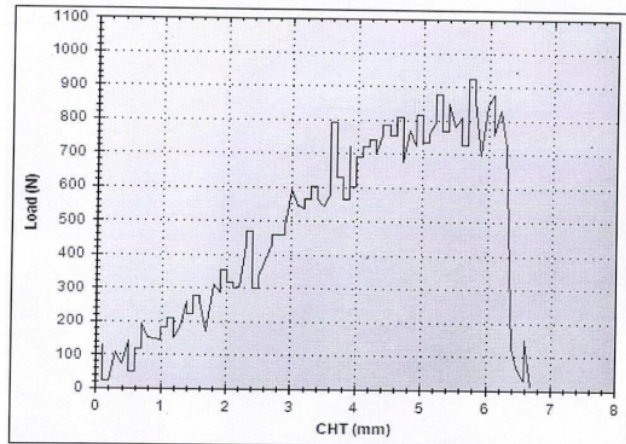


Graph 33 Experimental load- displacement graph of sample 17

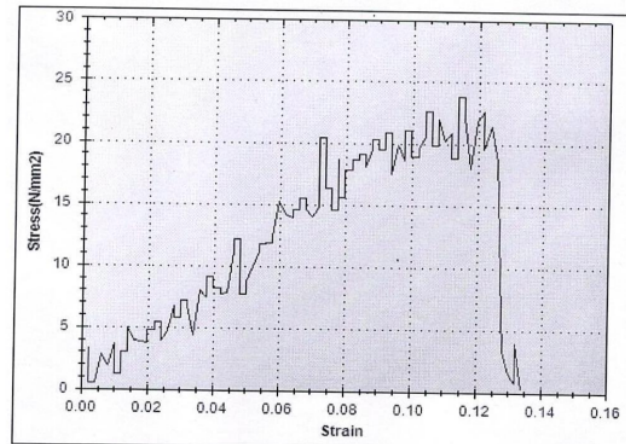


Graph 34 Experimental Stress- Strain graph of sample 17

| Gauge Length (in mm) | Final Gauge Length (in mm) | Peak Load (in N) | UTS (in MPa) | %age Elongation |
|----------------------|----------------------------|------------------|--------------|-----------------|
| 50 | 50.88 | 1047.5 | 26.706 | 1.76 |

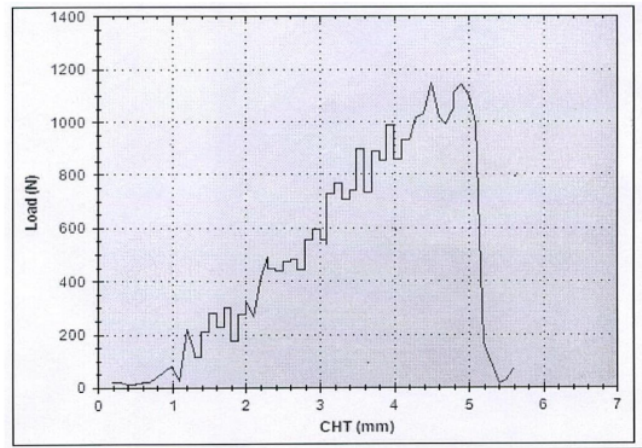


Graph 35 Experimental load- displacement graph of sample 18

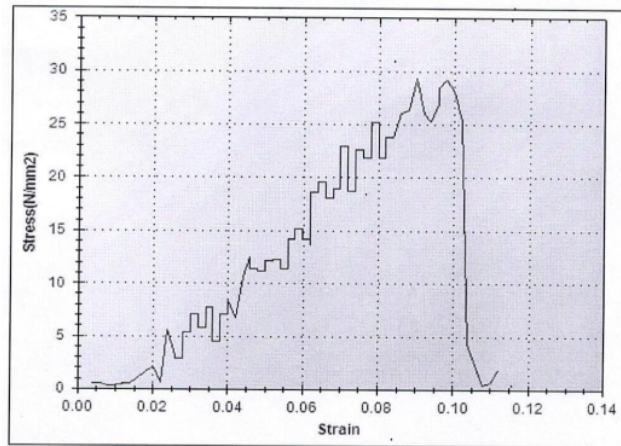


Graph 36 Experimental Stress- Strain graph of sample 18

| Gauge Length (in mm) | Final Gauge Length (in mm) | Peak Load (in N) | UTS (in MPa) | %age Elongation |
|----------------------|----------------------------|------------------|--------------|-----------------|
| 50 | 50.72 | 922.5 | 23.813 | 1.44 |

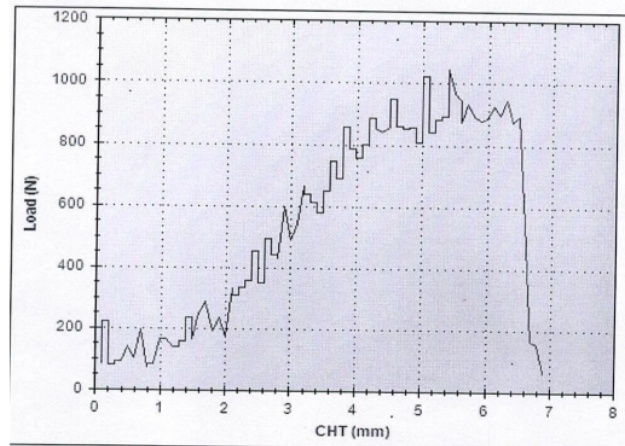


Graph 37 Experimental load- displacement graph of sample 19

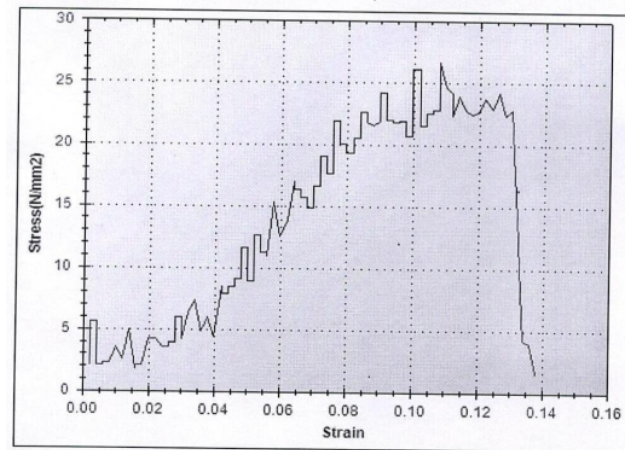


Graph 38 Experimental Stress- Strain graph of sample 19

| Gauge Length (in mm) | Final Gauge Length (in mm) | Peak Load (in N) | UTS (in MPa) | %age Elongation |
|----------------------|----------------------------|------------------|--------------|-----------------|
| 50 | 50.96 | 1145 | 29.283 | 1.92 |

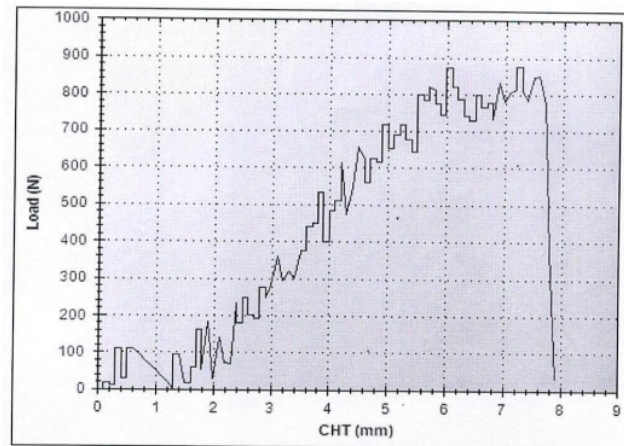


Graph 39 Experimental load- displacement graph of sample 20

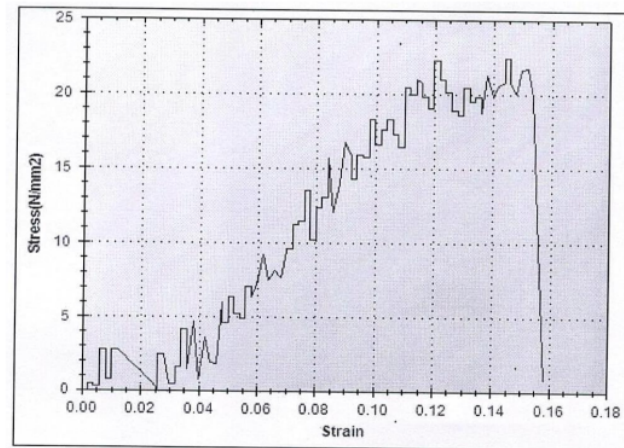


Graph 40 Experimental Stress- Strain graph of sample 20

| Gauge Length (in mm) | Final Gauge Length (in mm) | Peak Load (in N) | UTS (in MPa) | %age Elongation |
|----------------------|----------------------------|------------------|--------------|-----------------|
| 50 | 51.06 | 1042.5 | 26.62 | 2.12 |

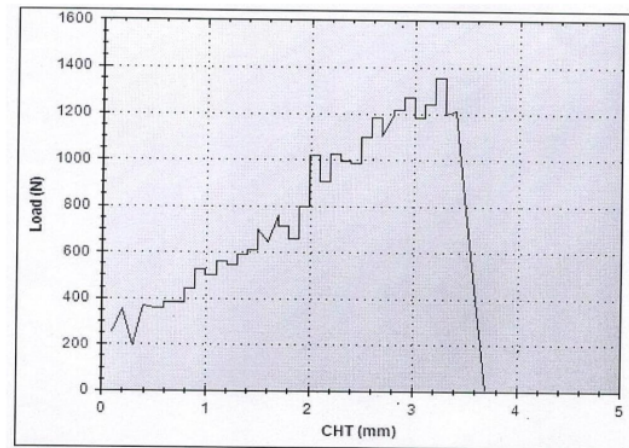


Graph 41 Experimental load- displacement graph of sample 21

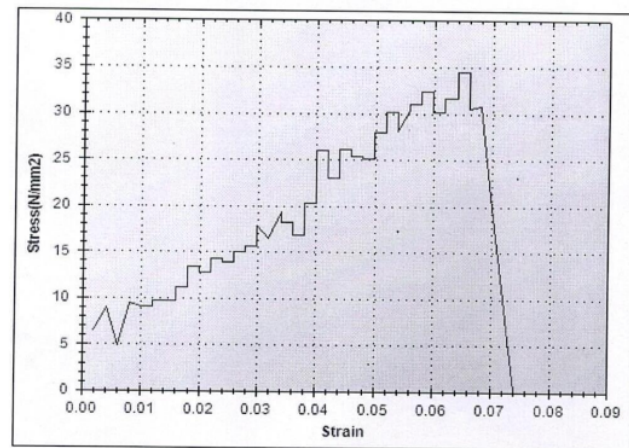


Graph 42 Experimental Stress- Strain graph of sample 21

| Gauge Length (in mm) | Final Gauge Length (in mm) | Peak Load (in N) | UTS (in MPa) | %age Elongation |
|----------------------|----------------------------|------------------|--------------|-----------------|
| 50 | 51.14 | 877.5 | 22.421 | 2.28 |

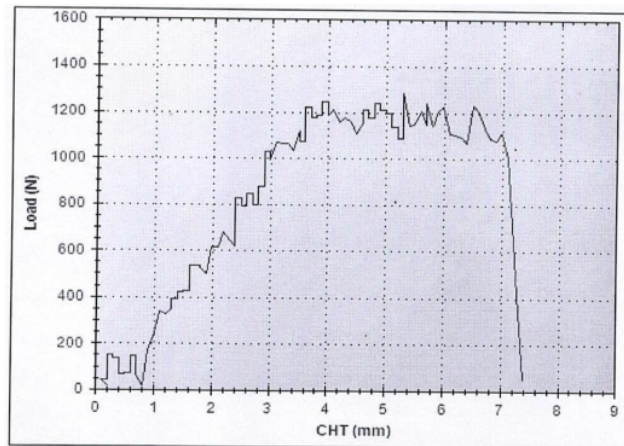


Graph 43 Experimental load- displacement graph of sample 22

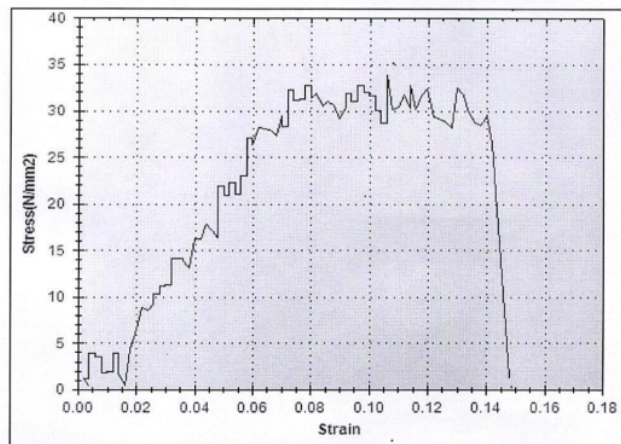


Graph 44 Experimental Stress- Strain graph of sample 22

| Gauge Length (in mm) | Final Gauge Length (in mm) | Peak Load (in N) | UTS (in MPa) | %age Elongation |
|----------------------|----------------------------|------------------|--------------|-----------------|
| 50 | 51.07 | 1355 | 34.492 | 2.14 |

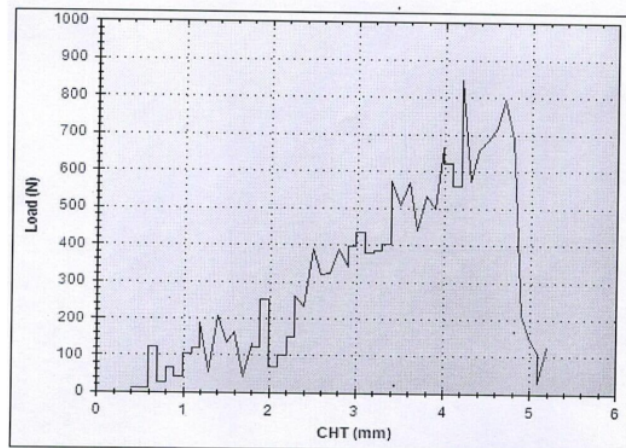


Graph 45 Experimental load- displacement graph of sample 23

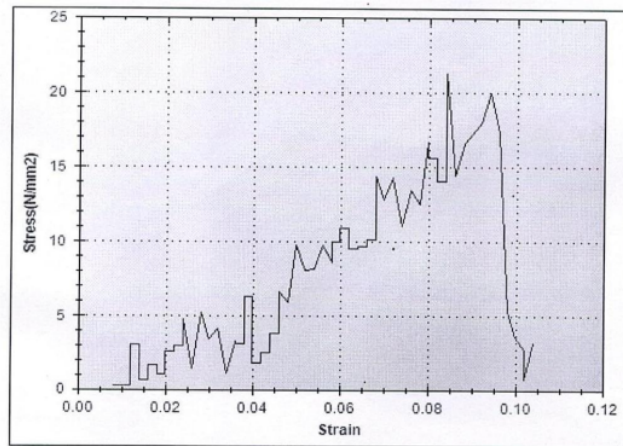


Graph 46 Experimental Stress- Strain graph of sample 23

| Gauge Length (in mm) | Final Gauge Length (in mm) | Peak Load (in N) | UTS (in MPa) | %age Elongation |
|----------------------|----------------------------|------------------|--------------|-----------------|
| 50 | 52.07 | 1282.5 | 33.826 | 4.14 |

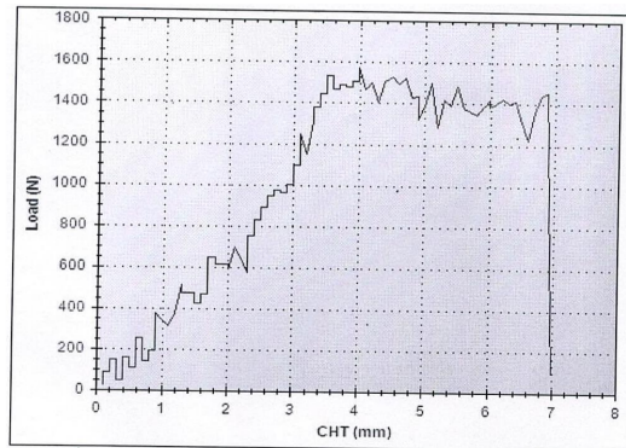


Graph 47 Experimental load- displacement graph of sample 24

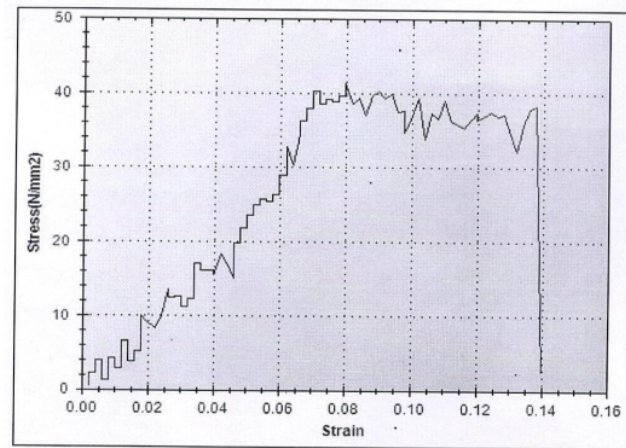


Graph 48 Experimental Stress- Strain graph of sample 24

| Gauge Length (in mm) | Final Gauge Length (in mm) | Peak Load (in N) | UTS (in MPa) | %age Elongation |
|----------------------|----------------------------|------------------|--------------|-----------------|
| 50 | 50.87 | 845 | 21.291 | 1.74 |

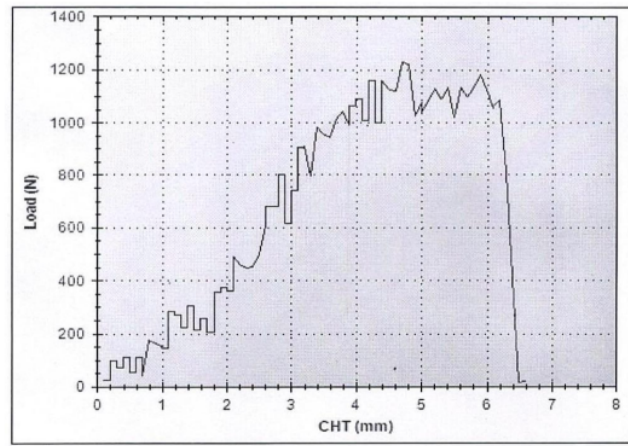


Graph 49 Experimental load- displacement graph of sample 25

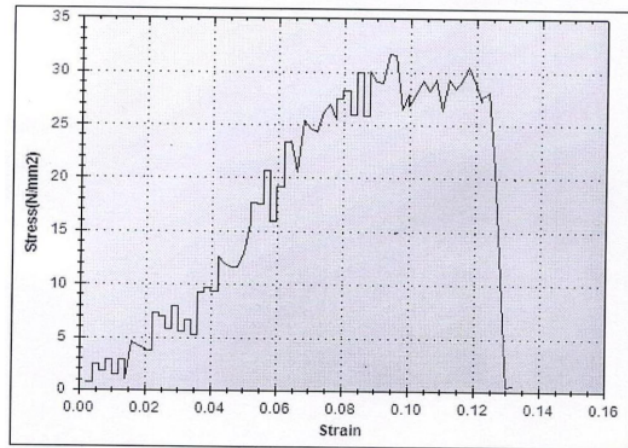


Graph 50 Experimental Stress- Strain graph of sample 25

| Gauge Length (in mm) | Final Gauge Length (in mm) | Peak Load (in N) | UTS (in MPa) | %age Elongation |
|----------------------|----------------------------|------------------|--------------|-----------------|
| 50 | 53.09 | 1570 | 41.32 | 6.18 |

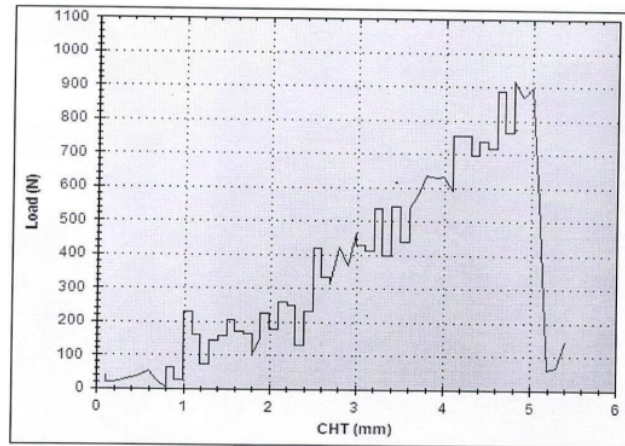


Graph 51 Experimental load- displacement graph of sample 26

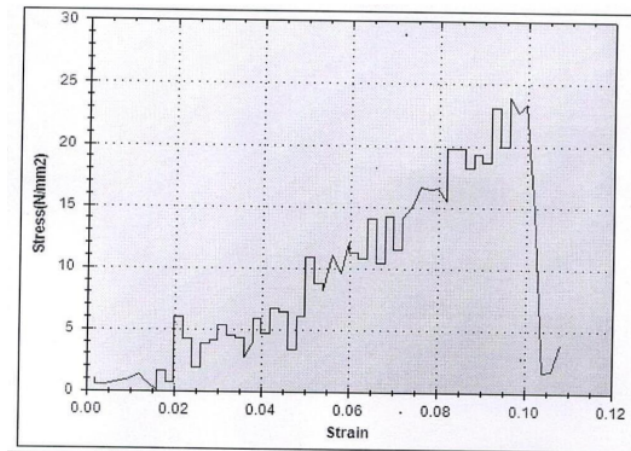


Graph 52 Experimental Stress- Strain graph of sample 26

| Gauge Length (in mm) | Final Gauge Length (in mm) | Peak Load (in N) | UTS (in MPa) | %age Elongation |
|----------------------|----------------------------|------------------|--------------|-----------------|
| 50 | 51.66 | 1225 | 31.661 | 3.32 |



Graph 53 Experimental load-displacement graph of sample 27



Graph 54 Experimental Stress- Strain graph of sample 27

| Gauge Length (in mm) | Final Gauge Length (in mm) | Peak Load (in N) | UTS (in MPa) | %age Elongation |
|----------------------|----------------------------|------------------|--------------|-----------------|
| 50 | 50.79 | 915 | 23.865 | 1.58 |

CHAPTER 5

ANALYSIS AND CALCULATIONS OF OPTIMUM VALUE

The specimens were manufactured with FFF 3-D printing and tested for tensile strength on a computerized universal testing machine (UTM). Artificial neural network technique is used to optimize the process parameters.

5.1 Taguchi Analysis

Taguchi analysis is carried out to obtain an optimal combination of parameter to maximize tensile strength of PLA component. The tensile strength of twenty-seven 3-D printed test specimens that were tested on the UTM is shown in Table 7. MINITAB 19 software was used to examine it. It is presumed that the study variables are unrelated and do not have influence on one another. After computing the Signal to Noise ratio for different levels of factors, the optimal combination is picked.

Table 7 Experimental Results

| Layer Thickness | Nozzle Temperature | Speed/feed rate | Structure | Raster orientation | UTS |
|-----------------|--------------------|-----------------|----------------|--------------------|--------|
| 100 | 190 | 40 | rectilinear | 0 | 44.118 |
| 100 | 190 | 40 | rectilinear | 45 | 27.269 |
| 100 | 190 | 40 | rectilinear | 90 | 14.329 |
| 100 | 200 | 50 | full_honeycomb | 0 | 33.605 |
| 100 | 200 | 50 | full_honeycomb | 45 | 24.278 |
| 100 | 200 | 50 | full_honeycomb | 90 | 19.956 |
| 100 | 210 | 60 | grid | 0 | 34.637 |

| | | | | | |
|-----|-----|----|----------------|----|--------|
| 100 | 210 | 60 | grid | 45 | 29.448 |
| 100 | 210 | 60 | grid | 90 | 17.143 |
| 150 | 190 | 50 | grid | 0 | 39.753 |
| 150 | 190 | 50 | grid | 45 | 33.496 |
| 150 | 190 | 50 | grid | 90 | 21.977 |
| 150 | 200 | 60 | rectilinear | 0 | 18.553 |
| 150 | 200 | 60 | rectilinear | 45 | 28.793 |
| 150 | 200 | 60 | rectilinear | 90 | 18.061 |
| 150 | 210 | 40 | full_honeycomb | 0 | 34.741 |
| 150 | 210 | 40 | full_honeycomb | 45 | 26.706 |
| 150 | 210 | 40 | full_honeycomb | 90 | 23.813 |
| 200 | 190 | 60 | full_honeycomb | 0 | 29.283 |
| 200 | 190 | 60 | full_honeycomb | 45 | 26.62 |
| 200 | 190 | 60 | full_honeycomb | 90 | 22.421 |
| 200 | 200 | 40 | grid | 0 | 34.492 |
| 200 | 200 | 40 | grid | 45 | 33.826 |
| 200 | 200 | 40 | grid | 90 | 21.291 |
| 200 | 210 | 50 | rectilinear | 0 | 41.32 |
| 200 | 210 | 50 | rectilinear | 45 | 31.661 |
| 200 | 210 | 50 | rectilinear | 90 | 23.865 |

Table 8 Response Table for Signal to Noise Ratios

| Levels | Layer Thickness | Nozzle Temperature | Speed/Feed Rate | Structure | Raster orientation |
|---------------|------------------------|---------------------------|------------------------|------------------|---------------------------|
| 1 | 28.20 | 28.77 | 28.84 | 28.26 | 30.53 |
| 2 | 28.43 | 27.98 | 29.27 | 28.44 | 29.24 |
| 3 | 29.18 | 29.07 | 27.71 | 29.12 | 26.05 |
| Delta | .98 | 1.09 | 1.56 | .86 | 4.40 |
| Rank | 4 | 3 | | 5 | 1 |

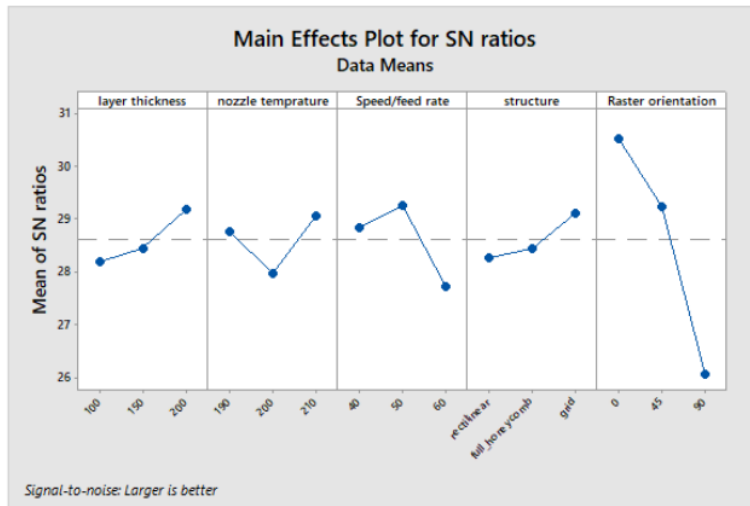


Figure 11 Main effects plot for S/N Ratios

Table 9 Response Table for Means

| Levels | Layer Thickness | Nozzle Temperature | Speed/Feed Rate | Structure | Raster orientation |
|--------|-----------------|--------------------|-----------------|-----------|--------------------|
| 1 | 27.20 | 28.81 | 28.95 | 27.55 | 34.50 |
| 2 | 27.32 | 25.87 | 29.99 | 26.82 | 29.12 |
| 3 | 29.42 | 29.26 | 25.00 | 29.56 | 20.32 |
| Delta | 2.22 | 3.39 | 4.99 | 2.74 | 14.18 |
| Rank | 5 | 3 | 2 | 4 | 1 |



Figure 12 Main effect for Means Plot using MINITAB

A clear trend was seen in the obtained stress data. By increasing the layer thickness, specimen tends to achieve the strength of a molded specimen. It is observed that temperature and speed have a similar trend. With increase in angle of raster orientation, tensile strength decrease. Out of different infill pattern of printing, grid shows maximum tensile strength. The process parameters for optimum tensile strength are below mentioned:

| | |
|--------------------------|-------------------|
| Layer Thickness | 200 μm |
| Nozzle Temperature | 210° C |
| Speed/Feed rate | 50 mm/min |
| Structure/infill pattern | Grid |
| Raster orientation | 0° |

5.2 Artificial Neural Network (ANN)



Figure 13 Structure of ANN developed using MATLAB

Figure 10 shows the regression plots, with R values near to 1 signifying that the minimum error was achieved. It also shows the training plot of ANN model. It indicates the numbers of training vectors are used once the weights are updated.

Table 10 Comparison of Experimental and ANN Predicted UTS Strength

| Layer Thickness | Nozzle Temperature | Speed/feed rate | structure | Raster orientation | UTS | Predicted UTS | Absolute Error |
|-----------------|--------------------|-----------------|-------------|--------------------|--------|---------------|----------------|
| 100 | 190 | 40 | rectilinear | 45 | 27.269 | 27.23109008 | 0.139022 |
| 100 | 190 | 40 | rectilinear | 0 | 44.118 | 44.43827584 | 0.725953 |
| 100 | 190 | 40 | rectilinear | 90 | 14.329 | 14.94267839 | 4.282772 |

| | | | | | | | |
|-----|-----|----|----------------|----|--------|-------------|----------|
| 100 | 200 | 50 | full_honeycomb | 45 | 24.278 | 24.36666664 | 0.365214 |
| 100 | 200 | 50 | full_honeycomb | 0 | 33.605 | 33.96590702 | 1.073968 |
| 100 | 200 | 50 | full_honeycomb | 90 | 19.956 | 20.1964672 | 1.204987 |
| 100 | 210 | 60 | grid | 0 | 34.637 | 34.69016339 | 0.153487 |
| 100 | 210 | 60 | grid | 45 | 29.448 | 29.19771696 | 0.849915 |
| 100 | 210 | 60 | grid | 90 | 17.143 | 17.62305755 | 2.800312 |
| 150 | 190 | 50 | grid | 45 | 33.496 | 33.19881825 | 0.887216 |
| 150 | 190 | 50 | grid | 0 | 39.753 | 39.20420292 | 1.380517 |
| 150 | 190 | 50 | grid | 90 | 21.977 | 22.32904582 | 1.601883 |
| 150 | 200 | 60 | rectilinear | 90 | 18.061 | 18.4560519 | 2.18732 |
| 150 | 200 | 60 | rectilinear | 45 | 28.793 | 29.42744173 | 2.203458 |
| 150 | 200 | 60 | rectilinear | 0 | 18.553 | 19.19194016 | 3.443864 |
| 150 | 210 | 40 | full_honeycomb | 45 | 26.706 | 26.78724075 | 0.304204 |
| 150 | 210 | 40 | full_honeycomb | 0 | 34.741 | 34.88558423 | 0.416178 |
| 150 | 210 | 40 | full_honeycomb | 90 | 23.813 | 23.01837485 | 3.336938 |
| 200 | 190 | 60 | full_honeycomb | 0 | 29.283 | 29.19038789 | 0.316266 |
| 200 | 190 | 60 | full_honeycomb | 45 | 26.62 | 26.85584661 | 0.885975 |
| 200 | 190 | 60 | full_honeycomb | 90 | 22.421 | 22.70997431 | 1.288856 |
| 200 | 200 | 40 | grid | 0 | 34.492 | 34.6710778 | 0.519186 |
| 200 | 200 | 40 | grid | 45 | 33.826 | 33.45842858 | 1.086654 |
| 200 | 200 | 40 | grid | 90 | 21.291 | 21.53682735 | 1.154607 |
| 200 | 210 | 50 | rectilinear | 90 | 23.865 | 23.74075807 | 0.520603 |
| 200 | 210 | 50 | rectilinear | 0 | 41.32 | 41.71543185 | 0.956999 |

| | | | | | | | |
|-----|-----|----|-------------|----|--------|-------------|----------|
| 200 | 210 | 50 | rectilinear | 45 | 31.661 | 31.24503686 | 1.313803 |
|-----|-----|----|-------------|----|--------|-------------|----------|

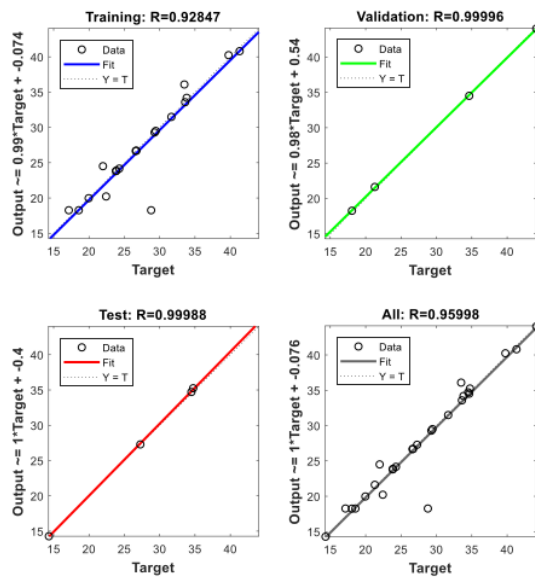


Figure 14 Regression plot of Artificial Neural Network

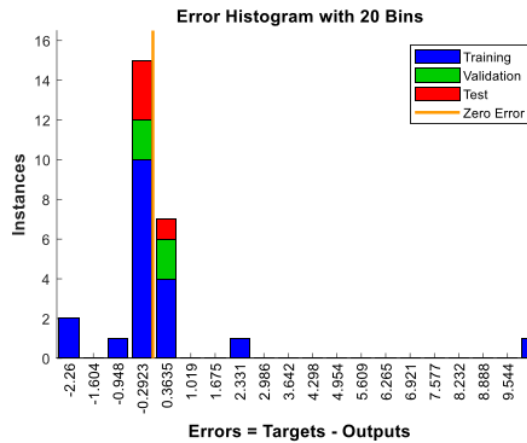


Figure 15 Error histogram

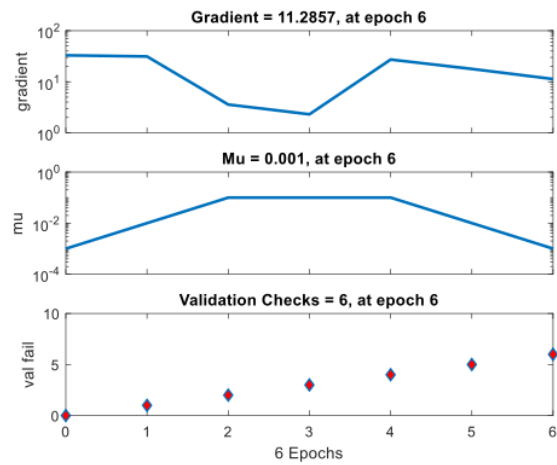


Figure 16 Training plot

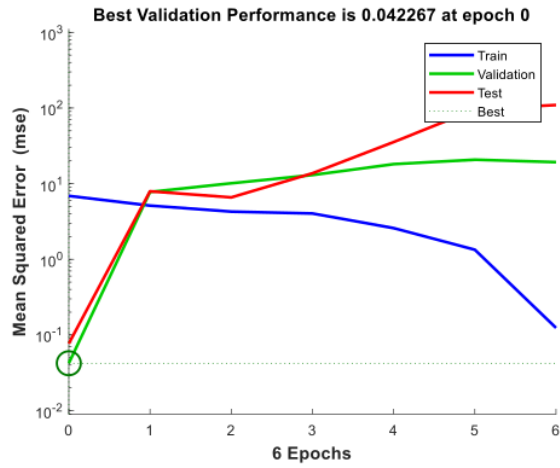


Figure 17 Performance plot

The ANN model is further used to predict the tensile strength of total 243 cases to find out optimum process parameters and the maximum tensile strength and the result is as follows: -

- Layer Thickness 200 μm
- Nozzle Temperature 210° C
- Speed/Feed rate 50 mm/min
- Structure/infill pattern Grid

- Raster orientation 0°
- Predicted UTS 52.68808667 MPA

CHAPTER 6

CONCLUSION

Additive manufacturing is one of the emerging fields that is revolutionizing manufacturing sector. To generate a component of consistent quality, it must understand the process parameters and their impact on the final built part. The impact of process factors on the tensile strength of the PLA material employed in this study was investigated. Some notable observations based on our experimental investigations carried out for process parameter optimization was that for the least change, layer thickness of 200 μm , nozzle temperature of 210° C, speed/feed rate of 50 mm/min, grid as a structure/infill pattern and raster orientation of 0° are required.

We have found that raster orientation has a significant effect on tensile strength and with increase in angle, tensile strength decreases. The specimen having fibre aligned along the loading direction have high tensile strength than other cases. Moreover, infill pattern or structure has also a great influence on tensile strength. The tensile strength of specimen is in order as grid followed by rectilinear, followed by full honeycomb. About high feed/ speed, tensile strength decreases as it does not give proper bonding time. Increasing feed helps in reducing build time but also resulted in poor surface finish and poor bonding. Also, with increase in layer thickness, tensile strength was found increased. Temperature has negative effect up to 200°C on tensile strength. Due to less temperature, bonding can't be done properly. But beyond 200°C, tensile strength of specimen was found increased. However, a thorough study is still required to get the better understanding the temperature dependence of the bonding process.

REFERENCES

1. Yi, L., C. Gläßner, and J.C. Aurich, *How to integrate additive manufacturing technologies into manufacturing systems successfully: A perspective from the commercial vehicle industry*. Journal of Manufacturing Systems, 2019. **53**: p. 195-211.
2. Ngo, T.D., et al., *Additive manufacturing (3D printing): A review of materials, methods, applications and challenges*. Composites Part B: Engineering, 2018. **143**: p. 172-196.
3. Kabir, S.F., K. Mathur, and A.-F.M. Seyam, *A critical review on 3D printed continuous fiber-reinforced composites: History, mechanism, materials and properties*. Composite Structures, 2020. **232**: p. 111476.
4. Pfähler, K., D. Morar, and H.-G. Kemper, *Exploring application fields of additive manufacturing along the product life cycle*. Procedia CIRP, 2019. **81**: p. 151-156.
5. Rajaguru, K., T. Karthikeyan, and V. Vijayan, *Additive manufacturing—State of art. Materials today: proceedings*, 2020. **21**: p. 628-633.
6. Dilberoglu, U.M., et al., *The role of additive manufacturing in the era of industry 4.0*. Procedia Manufacturing, 2017. **11**: p. 545-554.
7. Camacho, D.D., et al., *Applications of additive manufacturing in the construction industry—A forward-looking review*. Automation in construction, 2018. **89**: p. 110-119.
8. Javaid, M. and A. Haleem, *Current status and applications of additive manufacturing in dentistry: A literature-based review*. Journal of oral biology and craniofacial research, 2019. **9**(3): p. 179-185.
9. Zaldivar, R., et al., *Influence of processing and orientation print effects on the mechanical and thermal behavior of 3D-Printed ULTEM® 9085 Material*. Additive Manufacturing, 2017. **13**: p. 71-80.
10. Ertane, E.G., et al., *Processing and wear behaviour of 3D printed PLA reinforced with biogenic carbon*. Advances in Tribology, 2018. **2018**.
11. Williams, R., et al., *Investigation of the effect of various build methods on the performance of rapid prototyping (stereolithography)*. Journal of materials processing technology, 1996. **61**(1-2): p. 173-178.
12. Frank, D. and G. Fadel, *Expert system-based selection of the preferred direction of build for rapid prototyping processes*. Journal of Intelligent Manufacturing, 1995. **6**(5): p. 339-345.
13. Sood, A.K., R.K. Ohdar, and S.S. Mahapatra, *Experimental investigation and empirical modelling of FDM process for compressive strength improvement*. Journal of Advanced Research, 2012. **3**(1): p. 81-90.
14. Sexton, R.S., R.E. Dorsey, and J.D. Johnson, *Toward a Global Optimum for Neural Networks*. 1995, University of Mississippi Department of Economics and Finance.
15. Koch, C., L. Van Hulle, and N. Rudolph, *Investigation of mechanical anisotropy of the fused filament fabrication process via customized tool path generation*. Additive Manufacturing, 2017. **16**: p. 138-145.
16. Yin, J., et al., *Interfacial bonding during multi-material fused deposition modeling (FDM) process due to inter-molecular diffusion*. Materials & Design, 2018. **150**: p. 104-112.
17. Wang, J., et al., *A novel approach to improve mechanical properties of parts fabricated by fused deposition modeling*. Materials & Design, 2016. **105**: p. 152-159.
18. Abeykoon, C., P. Sri-Amphorn, and A. Fernando, *Optimization of fused deposition modeling*

- parameters for improved PLA and ABS 3D printed structures*. International Journal of Lightweight Materials and Manufacture, 2020. **3**(3): p. 284-297.
19. Afrose, M.F., et al., *Effects of part build orientations on fatigue behaviour of FDM-processed PLA material*. Progress in Additive Manufacturing, 2016. **1**(1): p. 21-28.
 20. Kamaal, M., et al., *Effect of FDM process parameters on mechanical properties of 3D-printed carbon fibre-PLA composite*. Progress in Additive Manufacturing, 2021. **6**(1): p. 63-69.
 21. Othman, F.M., T. Fadhil, and A.H.B. Ali, *Influence of process parameters on mechanical properties and printing time of FDM PLA printed parts using design of experiment*. Journal of Engineering Research. ISSN, 2018: p. 2248-9622.
 22. Omer, R., H.S. Mali, and S.K. Singh, *Tensile performance of additively manufactured short carbon fibre-PLA composites: neural networking and GA for prediction and optimisation*. Plastics, Rubber and Composites, 2020. **49**(6): p. 271-280.
 23. Rajpurohit, S.R. and H.K. Dave, *Effect of process parameters on tensile strength of FDM printed PLA part*. Rapid Prototyping Journal, 2018.
 24. Zhang, X., et al., *Effects of raster angle on the mechanical properties of PLA and Al/PLA composite part produced by fused deposition modeling*. Polymers for Advanced Technologies, 2019. **30**(8): p. 2122-2135.
 25. Rao, V.D.P., P. Rajiv, and V.N. Geethika, *Effect of fused deposition modelling (FDM) process parameters on tensile strength of carbon fibre PLA*. Materials Today: Proceedings, 2019. **18**: p. 2012-2018.
 26. Srinivasan, R., et al., *Impact of fused deposition process parameter (infill pattern) on the strength of PETG part*. Materials Today: Proceedings, 2020. **27**: p. 1801-1805.
 27. Agatonovic-Kustrin, S. and R. Beresford, *Basic concepts of artificial neural network (ANN) modeling and its application in pharmaceutical research*. Journal of pharmaceutical and biomedical analysis, 2000. **22**(5): p. 717-727.
 28. Bayraktar, Ö., et al., *Experimental study on the 3D-printed plastic parts and predicting the mechanical properties using artificial neural networks*. Polymers for Advanced Technologies, 2017. **28**(8): p. 1044-1051.

Thesis

ORIGINALITY REPORT

9%

SIMILARITY INDEX

5%

INTERNET SOURCES

4%

PUBLICATIONS

6%

STUDENT PAPERS

PRIMARY SOURCES

- | | | |
|---|---|----|
| 1 | Submitted to University of Melbourne Student Paper | 1% |
| 2 | Submitted to Delhi Technological University Student Paper | 1% |
| 3 | "Advances in Manufacturing and Industrial Engineering", Springer Science and Business Media LLC, 2021 Publication | 1% |
| 4 | Meena Pant, Ranganath M Singari, Pawan Kumar Arora, Girija Moona, Harish Kumar. "Wear assessment of 3-D printed parts of PLA (polylactic acid) using Taguchi design and Artificial Neural Network (ANN) technique", Materials Research Express, 2020 Publication | 1% |
| 5 | Submitted to Delhi University Student Paper | 1% |
| 6 | espace.aus.edu:8443 Internet Source | 1% |
| 7 | Submitted to Engineers Australia | |

Student Paper

<1 %

8

libgen.mkxa.top

Internet Source

<1 %

9

K. Rajaguru, T. Karthikeyan, V. Vijayan.
"Additive manufacturing – State of art",
Materials Today: Proceedings, 2020

Publication

<1 %

10

dspace.dtu.ac.in:8080

Internet Source

<1 %

11

Submitted to Kingston University

Student Paper

<1 %

12

Submitted to ESCP-EAP

Student Paper

<1 %

13

eprints.nottingham.ac.uk

Internet Source

<1 %

14

Submitted to University of Sheffield

Student Paper

<1 %

15

Annamaria Gisario, Michele Kazarian,
Filomeno Martina, Mehrshad Mehrpouya.
"Metal additive manufacturing in the
commercial aviation industry: A review",
Journal of Manufacturing Systems, 2019

Publication

<1 %

- | | | |
|----|--|------|
| 16 | Wei Gao, Yunbo Zhang, Devarajan Ramanujan, Karthik Ramani et al. "The status, challenges, and future of additive manufacturing in engineering", Computer-Aided Design, 2015 Publication | <1 % |
| 17 | www.i-scholar.in Internet Source | <1 % |
| 18 | www.springerprofessional.de Internet Source | <1 % |
| 19 | repository.christuniversity.in Internet Source | <1 % |
| 20 | www.omicsonline.org Internet Source | <1 % |
| 21 | upcommons.upc.edu Internet Source | <1 % |
| 22 | Kathrin Pfähler, Dominik Morar, Hans-Georg Kemper. "Exploring Application Fields of Additive Manufacturing Along the Product Life Cycle", Procedia CIRP, 2019 Publication | <1 % |
| 23 | V. Durga Prasada Rao, P. Rajiv, V. Navya Geethika. "Effect of fused deposition modelling (FDM) process parameters on tensile strength of carbon fibre PLA", Materials Today: Proceedings, 2019 | <1 % |

24 Zaragoza-Siqueiros, Jorge, and Hugo I. Medellín-Castillo. "Design for Rapid Prototyping, Manufacturing and Tooling: Guidelines", Volume 2A Advanced Manufacturing, 2014.

Publication

<1 %

25 erepository.uonbi.ac.ke

Internet Source

<1 %

26 jpier.org

Internet Source

<1 %

27 mro.massey.ac.nz

Internet Source

<1 %

28 uwe-repository.worktribe.com

Internet Source

<1 %

29 www.scribd.com

Internet Source

<1 %

30 "Fused Deposition Modeling Based 3D Printing", Springer Science and Business Media LLC, 2021

Publication

<1 %

Exclude quotes Off

Exclude matches Off

Exclude bibliography On